Title
Addressing channel incision through floodplain reconnection: Revisiting the Lower Tassajara Creek project

Author
Lewis, Skyler

Publication Date
2023-10-13

PRELIMINARY REPORT

Addressing channel incision through floodplain reconnection:

Revisiting the Lower Tassajara Creek project

Skyler Lewis
LA227 Restoration of Rivers and Streams
December 2022

Abstract

Actively incising Lower Tassajara Creek in Dublin, California, was restored as a compound channel in 1999-2000 to mitigate incision and provide flood conveyance capacity to reduce flood risk to an adjacent greenfield residential development. The project benefitted from a wide floodplain corridor set aside during development, allowing a rough vegetated overbank channel with a design capacity to carry the 100-year flood. Several years of cross-sectional channel surveys conducted under an informal monitoring program from 2000 to 2006 indicated that active incision was largely attenuated following the restoration, with some minor incision still evident and low-flow channel complexity just beginning to develop. This research evaluates Lower Tassajara Creek 20 years after its restoration, investigating ongoing channel evolution, incision and aggradation, and floodplain reconnection, and discussing channel conditions in the context of the catchment land use history. I repeated and overlayed a series of cross-section surveys to detect channel incision and overbank deposition, documented field observations of channel condition, and cross-referenced against LiDAR terrain data to detect depositional landforms on the floodplain. I also developed a one-dimensional hydraulic model to better understand current flood conveyance capacity, using channel roughness back-calculated using measured high water marks from a recent storm. Preliminary results suggest overbank deposition has occurred in some locations, particularly in the upper reaches, while shallow slopes and fine sediment in the low flow channel throughout the project indicate a depositional environment. While active incision appears to have halted, entrenched conditions persist in the reach with a deeper low-flow channel sized to carry the 5-year flow. There may be opportunities to improve floodplain connection by adding woody debris to push more frequent flows out of the low flow channel, but additional hydraulic model validation and testing will be required to determine where flood conveyance capacity is sufficient to support such an intervention.

Introduction

Incision and Floodplain Disconnection

Stream channel incision, the erosion and lowering of the stream channel bed, may be caused by an increase in the energy of the stream (through steepening or introduction of a flashier flow regime), a change in sediment flux (e.g. less sediment entering from upslope), or a decrease in the resistance of the channel (e.g. by removal of vegetation) (Schumm, 1999). Alterations to flow and sediment regimes are frequently brought about by climatic changes or catchment changes including damming, timber harvesting, grazing, urbanization, and other land use changes.

Entrenched stream channels can cause undermining of hillslopes, bridges, pipelines, and other infrastructure. The changing channel geometry (decreasing width-depth ratio) is likely to reduce the area and diversity of in-stream aquatic habitat. Channels are simplified, side channels are abandoned, and complex channel margins offering shelter and feeding opportunities are eliminated (Bravard et al., 1999). Channel incision can be self-reinforcing, as the incised channel's concentrated flows cause more erosion and downcutting, and will often propagate upward in the stream channel (Haltiner & Beeman, 2003, p. 212).

Channel incision disconnects a stream from its adjacent floodplain in both the lateral and vertical dimensions. Incision reduces overbank flood frequency, which compromises the critical ecological and geomorphic functions provided by flood pulses (Junk et al., 1989; Middleton, 2002). Many riparian plants rely on periodic lateral flood pulses to disperse seeds, colonize freshly deposited sediment, and receive nutrients. High-magnitude floods create a complex mosaic of successional communities by scouring roots, breaking stems, and creating new habitat through lateral channel migration and avulsion (Stella et al., 2013). Incision also drops the water table beneath the floodplain, reducing groundwater storage (Bravard et al., 1999) and putting water out of reach of vegetation. Phreatophytic riparian vegetation in Mediterranean riparian ecosystems overcome seasonal drought by tapping perennial groundwater (Stella et al., 2013); dropping water tables creates an effective hydrological drought (Groffman et al., 2003) that can cause desiccation especially in young seedlings with shorter roots (Stella et al., 2013).

Schumm (1984) and Simon & Hupp (1986)'s classical channel evolution models predict that over time, an incising channel will undergo a sequence of bank erosion, channel widening, and aggradation, eventually restabilizing into a single-threaded channel on an inset floodplain. In incising coastal California streams, however, it is common for streams to never reach this stable

quasi-equilibrium, owing to the flashy, episodic Mediterranean-climate hydrology. Instead, consolidating gullies and head cuts may push a recovering channel back into the active incision phase, flushing out sediment and recovered bedforms and cutting the channel deeper (Haltiner & Beeman, 2003). This process may prevent coastal California streams from naturally recovering their floodplain connectivity once it is lost due to watershed flow and sediment change. Cluer and Thorne (2014) account for this "short-circuit" in the loop back from Stage 4 to Stage 3 in their revised stream evolution model.

Floodplain Reconnection

Floodplain reconnection projects address the ecological degradation of leveed or incised channels by forcing the channels to spill out onto existing or constructed floodplains. Reconnection approaches for incised channels include raising the channel to its restored floodplain elevation, or excavating a new floodplain to create a compound channel at the lower elevation (Haltiner & Beeman, 2003).

Designing a floodplain reconnection project requires first evaluating the causes and controls of disconnection through analysis of the watershed's hydrologic and sediment regime (Beechie et al., 2010; Haltiner & Beeman, 2003). A channel may be incised due to historical catchment conditions, or the present catchment conditions may be continuing to produce active incision. The range of possible interventions to address the disconnection depends on natural factors such as local litho-topographic controls (Beechie et al., 2010), flow and sediment regimes, and riparian ecologies, as well as social factors, namely the availability of adjacent land in the corridor. Interventions that promise longer flood residence time and stronger ecological benefits often require wider corridors (Serra-Llobet et al., 2022).

Urban sites differ from rangeland and wildland sites in their constraints as well as their opportunities. More funding is available for urban floodplain restoration projects packaged as multi-benefit flood control projects. Available corridor width, however, is a key constraint for any project increasing the hydraulic roughness of a floodway, and urban land values limit the ability to acquire additional land. Urbanizing areas undergoing greenfield development offer the possibility of wider corridors where existing land use and infrastructure conflicts do not exist (Haltiner & Beeman, 2003). However, both urbanized and newly-urbanizing areas will face the range of impediments to successful ecological restoration known as "urban stream syndrome" (Walsh et al., 2005), including flashy runoff from impervious catchments (Wolman, 1967), perennial poor-quality water inputs or "urban slobber" (Kondolf et al., 2013), and risk of acute, catastrophic water quality impacts. Politically, there is more risk aversion to experimenting with

new floodplain reconnection strategies in a multi-benefit flood control project than in a wildland ecosystem project (Haltiner & Beeman, 2003), although where flood conveyance capacity allows, the opportunities for visibility and public recreational access are unmatched.

Compound Channel Restoration

Due to the confluence of these factors, compound channels have become a popular strategy for floodplain reconnection in urban areas, particularly in urbanizing areas undergoing greenfield development. Constructed compound channels allow a longer residence time and have more potential ecological benefits than engineered channels, and have lower corridor width requirements than natural floodplain reconnection strategies (Serra-Llobet et al., 2022).

Compound channels, also known as two-stage channels, consist of a low-flow channel containing the "normal range of flows" that is inset "within a larger channel constructed above bank-full by widening out the floodplain" (Brookes, 1989). The compound channel maintains the riverbed at its incised level: it is adapting the site to the modified, post-incision long profile of the river, rather than restoring its original level (Haltiner & Beeman, 2003). The inset channel allows for perennial fish passage and prevents deposition of sediment at very low flows, while the adjacent floodplain bench permits the required conveyance of flood waters at high flows. Where allowable per conveyance requirements and ecological support, the floodplain bench may host a full riparian forest community, or it may be restricted to herbaceous vegetation to minimize hydraulic roughness (Brookes, 1989). Constructing a compound channel involves the excavation of large amounts of material which must be placed onsite or nearby (e.g. for construction project fill in urbanizing areas or to supplement adjacent fields in agricultural areas) (Haltiner & Beeman, 2003).

The choice of low flow channel capacity is a critical design decision for compound channel projects. Current practice sets the low flow channel discharge between the 1.5-year and 5-year flow. In a low-capacity 1.5-year low flow channel, the lack of shading in early years may allow emergent vegetation to establish in the low flow channel, reducing capacity and leading to overbanking and new channel formation on the floodplain (Haltiner et al., 1996). While in the unconstrained restoration context, this could be taken as a sign of successful floodplain reconnection (Beechie et al., 2010; Ciotti et al., 2021), the reduced capacity may present a problem in the constrained urban flood control channel environment. On the other hand, a higher-capacity low flow channel exceeds the return interval for floodplain activation flows (Williams et al., 2009). Tompkins and Kondolf (2007) observed persistent incised conditions in

the section of Tassajara Creek with a 5-year capacity low flow channel, and improved floodplain reconnection in the section with a 1.5-year capacity low flow channel.

Stage Zero Restoration

The expense of channel reconstruction typically limits rehabilitation projects to individual reaches within broader, still-degraded systems. Allowing natural recovery, however, has a long lag time (Brookes et al., 1996). Low-cost and quickly deployable solutions involving large woody debris (LWD) and beaver dam analogues (BDAs) have gained traction in wildland and rangeland stream restoration. Growing evidence suggests that colonial-era conversion of streams from multi-threaded wet meadow systems to single-threaded channels was even more widespread than previously understood (Walter & Merritts, 2008). Cluer and Thorne's (2014) updated channel evolution model, which considers multi-threaded wet meadow systems to be the ultimate equilibrium state, has informed "stage zero" (Bowles et al., 2021) restoration frameworks that aim to "reset" the riverbed and allow natural fluvial processes to determine the future channel course (Bowles et al., 2021). By slowing and obstructing flows, in-stream placement of wood structures can accelerate both channel widening and sediment accumulation, raising the streambed until it reconnects to its former floodplain (Pollock et al., 2014) and promoting recovery from a single, entrenched channel into a multi-channel or wet meadow system. While stage zero restoration has been practiced to much success in wildland and rangeland stream restoration, the restoration of natural aggradation and avulsion processes tends to run up against conveyance concerns in flood-control oriented urban contexts where right-of-way is often limited.

Study Site

Tassajara Creek drains a 26.5 mi^2 catchment on a south-facing slope of the Mount Diablo foothills, originating in the Black Hills near the Morgan Territory preserve (Figure 1). South of Interstate 580, the creek flows into Arroyo Mocho, which crosses laterally through the Livermore and Amador Valleys, and then flows to the San Francisco Bay by way of Arroyo de la Laguna and Alameda Creek. Owing to the area's Mediterranean climate, the creek has seasonal baseflow and experiences episodic high floods during winter storms. Its upstream catchment is mostly rangeland with scattered rural development, while areas adjacent to the project reach in the Amador Valley are increasingly built-up.

In the 1990s, the City of Dublin, California planned for eastward greenfield expansion into the land surrounding Lower Tassajara Creek (Figure 2). The creek crossed through a military

base adjacent to a naval hospital; after the base closure, the land on both sides of the creek was turned over to Alameda County and sold for redevelopment. The creek channel was suffering from incision (Figure 3) likely triggered by 19th-century cattle grazing, which had increased surface runoff into the stream by reducing stabilizing vegetative cover and compacting soils. The restoration of Lower Tassajara Creek, concurrent with housing development, promised to stabilize the creek banks by curbing incision, to provide flood protection to the adjacent homes, and to create a new greenway amenity for the neighborhood.

Under its compound or two-stage channel design, the existing channel bottom was mostly kept in place as a low-flow channel with a wide floodplain bench excavated out at either side. The base level of the stream remained at its incised elevation, but high flows would spill out of the inner channel onto the floodplain while still remaining safely contained within the larger floodway. Because of the concurrent development of neighborhood and creek, a wide enough corridor was set aside to hydraulically support a full riparian forest community on the floodplain benches, which vegetated substantially over the subsequent years (Figure 4). The project design varied across three distinct reaches (Figure 5), with low flow channel capacities ranging from 2-year capacity (lower reach) to 5-year flow capacity (middle reach) and a multi-channel design in the upper reach.

Catchment Conditions and Historical Ecology

Lower Tassajara Creek once ran through a seasonally-flooded alkali wet meadow ecosystem and drained into a vast freshwater marsh. Three subsequent rounds of hydrologic modification—Mexican land grant *ranchos*, post-statehood farming and grazing, and postwar suburban development—have transformed wet meadows into dry uplands and caused the creek channel to incise and disconnect from its former floodplain. Understanding the history of channel incision is critical to contextualize the 21st century restoration project and today's watershed processes.

Historical ecology

The alluvial basin of the Livermore-Amador Valley was once a mosaic of freshwater marsh ecosystems referred to collectively as the Pleasanton Marsh Complex (Figure 6). Wetlands extended 2,600 acres perennially and up to 10,000 acres seasonally, with a northern border coinciding with today's Interstate 580. Reconstructions from early Spanish and Mexican land grant *diseño* maps indicate a perennial pond (*laguna*) at the lowest portion of the basin, surrounded by freshwater tule marsh (*tulare*) and willow thicket (*sausal*). Seasonal inundation extended into wet meadow and alkali wet meadow (*salitroso*) habitat, with high water retention

due to poorly-drained clay-rich soils, that transitioned into upland grassland. Habitat boundaries were a complex patchwork and extents varied across wet and dry years (Stanford et al., 2013, p. 89). High groundwater levels produced artesian wells on the slopes of the alluvial fan. In the hills above the marsh, land cover was grassland punctuated by occasional low-density clusters of oaks. However, dense riparian forest—primarily oak and sycamore—was present along larger streams (Stanford et al., 2013, p. 104).

Tassajara Creek was a single-threaded channel, running from upslope woodlands and grasslands through seasonally-saturated wet meadows around what is now the restoration project reach. The top of the project reach is located near the head of the Amador Valley alluvial fan, where the fan meets sedimentary bedrock[1] (Figure 7a). In contrast to the highly permeable gravel alluvial fans of the lower valley floor, the foothill soils underlying Tassajara Creek near this boundary are clay-rich (Figure 7b). This low-permeability soil keeps water near the surface and supports seasonal herbaceous freshwater emergent wetland, particularly alkali meadows with high residual salt content, and "occasional oak and sycamore trees or clumps of willows" (Stanford et al., 2013, p. 101).

Near today's Interstate 580 crossing, the stream entered a dense willow thicket sink at the periphery of the marsh complex. Around this location, it joined together with Arroyo Las Positas, though the exact location of the confluence varied. Tassajara Creek maintained a defined channel farther downstream than did many other northern tributaries, which tended to infiltrate into the alluvium or distribute into the marsh. However, its channel became very shallow downstream where it reached the willow thicket, frequently flooding and depositing fine sediment. The creek had perennial flow in the hills but intermittent flow where it reached the alluvial valley.

Land use change in the ranching era

The Mexican land grant era initiated a series of hydrologic and sediment regime changes that would impact channel form at both the watershed and reach scales. Lower Tassajara Creek[2] crosses from the former Rancho San Ramon (which extended through much of San Ramon Valley and its foothills), into Rancho Santa Rita (the alluvial lowlands of what is now Dublin and

[1] Upper and lower Cretaceous marine sedimentary bedrock underlies the headwater area. The Tassajara Anticline and Sycamore Syncline (Unruh et al., 2007) form steep linear topography at the Black Hills in the northwest of the catchment, near where this bedrock meets Domengine and San Pablo Group sandstones. The lower hills are Contra Costa Group and Tassajara Formation sandstone into which Tassajara Creek and its tributaries have laid down stream terrace deposits.

[2] Originally named *Tasajero* or *Tasajera*, referring to a place where, under Spanish tradition and in California's *rancho* era, beef would be hung to sun-dry into *carne seca* or *charqui* (Lane, 2006).

northern Pleasanton). These rancho lands were granted by the governor of Alta California in 1833 and 1839 respectively. The border is located around present-day Interstate 580 and at the former northern extent of the Pleasanton marsh complex.

Like many coastal California streams (Haltiner & Beeman, 2003), the channel was subject to an increase in surface runoff from intensive cattle grazing that began in this era, initiating a cycle of rapid and persistent channel incision (i.e., Cluer & Thorne, 2014, stages 3 and 4). Over-grazing eliminated the vegetative cover that previously slowed down overland flows in the catchment. Grazing also compacted the soil, reducing infiltration rates. Additionally, direct trampling along the river margins destabilized the banks (Haltiner & Beeman, 2003).

While cattle grazing transformed the uplands, the lowlands were reclaimed for row crops. Drainage of the Pleasanton marsh complex began in the 1800s, beginning with small modifications around the margins and escalating into rapid conversion by the early 1900s. Former distributary channels were confined to ditches and water was redirected for municipal use. In its heyday the Lower Tassajara watershed was considered a major "hay shed;" crops included alfalfa, hay, and grain to feed the growing dairy industries in the Fremont and Newark area, as well as sugar beets, flowers, and hops (Stanford et al., 2013, p. 51).

As early as 1972, Lower Tassajara Creek was ditched and straightened from the Rancho Santa Rita border to the confluence with Arroyo Las Positas (Figure 8). Testimonials indicate that it continued to overtop its banks and accumulate sediment (Stanford et al., 2013, p. 122). Drainage ditches in the Amador Valley continued to frequently overflow and accumulate sediment into the early 1900s while the water table in the valley remained high (*ibid.*). With the already-incising channel now confined to its banks, and a base level dropping from the pumping of the Amador Valley water table, steeper and faster flows probably initiated further incision that propagated upward.

The catchment today

By the time suburban growth exploded in the Amador and Livermore Valleys in the 20th century, the Pleasanton Marsh had been re-routed into a series of earthen channels. The largely-channelized Arroyo Mocho laterally traverses the alluvial plain—joining up with Arroyo Las Positas, Tassajara Creek, and other tributaries—to meet a channelized Arroyo de la Laguna that drains the entire basin into Alameda Creek.

In many similar coastal California streams (Haltiner & Beeman, 2003), catchment urbanization brought about another round of channel incision, as impervious surfaces created

flashy storm flows and reduced sediment inputs. In the case of Lower Tassajara Creek, the effect of urbanization may be attenuated compared to adjacent streams like Alamo Creek that have more impervious catchments.

While the Livermore-Amador Valley lands, including those adjacent to Lower Tassajara Creek, have undergone extensive redevelopment over recent decades, the upper catchment of Tassajara Creek remains a combination of agricultural open space and low-density rural residential. Most of the catchment is in Contra Costa County and sits almost entirely outside the county's Urban Limit Line. According to the California Protected Areas Database, 4961 acres are currently protected open space or conservation easements, accounting for 29% of the catchment area (Figure 9).

A higher proportion of the land is built out in the lower catchment within Alameda County. The effective catchment is extended in places by the piped storm drain network, while in other places, flows within the hydrologic catchment are piped away into Chabot Canal to the west or directly into Arroyo Mocho (Figure 10). The additional impervious surface area added to the catchment may contribute to flashier flows (Dunne & Leopold, 1978) for the Lower Tassajara Creek hydrograph.

Site Conditions

The Lower Tassajara Creek restoration site consists of distinct reaches along a 200- to 300-foot-wide flood corridor, each implementing a distinct restoration design and planted with a now-mature riparian tree and shrub community (Figure 5). The southern reach from Interstate 580 to Dublin Blvd was completely reconstructed as a compound channel: a wide trapezoidal channel designed to carry 100-year flood levels is inset with a new meandering low flow channel designed for the 2-year flow. The northern reach from Dublin Blvd to Gleason Dr maintained most of its original channel, with a wide 100-year floodplain terrace constructed past the 15-year flood line. The low-flow channel is rated to contain the 5-year flood. In two locations, the low-flow channel was rerouted to preserve the root structure of old-growth valley oaks. At the northern end of this section, a meander bend was constructed with the original oak-lined channel repurposed as an overflow swale, while farther south, the overbank floodplain is narrowed to avoid tree roots.

Aside from the old-growth valley oaks, most vegetation was freshly planted for the restoration project, and the site has grown in substantially over the following two decades. Residents are no longer able to see across the channel to neighborhoods across the way (Figure 11), nor to see water in the channel from most publicly accessible routes. A single location

provides vertical public access from the trail down to the low flow channel: a seasonal footpath open June through September and inundated in the rainy season. Otherwise, the stream corridor below street level is entirely off limits. Because of the capacity of the low flow channel, water would only be seen on the higher terraces during the occasional storm.

In the northern reach, neighbors can access the site along longitudinal recreation trails, some of which double as maintenance roads. Some of the trails are designated as part of a regional recreation trail system, while others are signed for local access. The northeast trail adjacent to Emerald Glen Park—which was developed after the restoration project—is the section of trail with the most public usage. Subjectively, this area is also the most attractive: valley oaks, arroyo willows, and variable topography add to the visual interest and make the site more of a riparian forest than an earthen flood control channel. Flocks of wild turkeys frequent the terraces while egrets can be seen in the low flow channel.

The southern reach below Dublin Blvd, in contrast, is closed to the public and has no adjacent trail access; this section serves entirely as a flood control corridor without the community parkland co-benefits. The adjacent land use consists of car dealerships and auto maintenance shops rather than neighborhoods and parks. This section tends to have the highest presence of homeless individuals camping out in the overbank terrace area, as well as in the trapezoidal channel below Interstate 580 to the south. As a result, this area receives the most frequent maintenance to remove buildup of scrubby underbrush and maintain visibility. Lush wetland vegetation in the wet season gives way to a dry and desolate appearance in the dry season.

A series of informal geomorphic (Hudzik & Truitt, 2001; Krofta & Novotney, 2003; Tompkins, 2006; Butler & Nolan, 2007) and vegetation (Trinh & Percelay, 2008) monitoring studies conducted during the first decade after project completion indicated substantial growth of floodplain riparian forest and mostly stable channel conditions. While active incision appeared to have stopped, portions of the creek with higher-capacity (5-year) low-flow channels remained in a degraded state with minimal overbank connectivity to the floodplain (Tompkins & Kondolf, 2007). A hydraulic modeling study (Chan & Heard, 2006) used high water marks deposited by the 20-year storm that took place on 30-31 December 2005 to back-calculate hydraulic roughness for six cross-sections, and determined that overbank roughness varied substantially by cross-section but remained within the design specification of n=0.120.

Methods

Field surveys

From April through September 2022, I conducted a series of cross-sectional surveys based on the alignments established for the informal Tassajara Creek monitoring program by Hudzik and Truitt (2001). Locating the precise alignments required consulting documentation from subsequent monitoring reports (Krofta & Novotney, 2003; Butler & Nolan, 2007), approximate GPS coordinates conducted during prior surveys, and georeferenced design drawings (Brian Kangas Foulk Engineers, 1999). I compiled documentation of the current best-available knowledge of endpoints for each section.

Of the eight cross sections established by Hudzik and Truitt (2001), I re-surveyed the six that were surveyed by Tompkins (2006) and used for hydraulic modeling by Chan & Heard (2006). These six cross sections (Table 1) are distributed throughout the Tassajara Creek reach, spanning the northern multi-channel reach (cross section B), the middle 5-year channel reach (cross sections D, E, F), and the southern 2-year channel reach (cross sections G, H) (Figure 5). For each section, my survey team and I cleared brush to establish access and line of sight, then conducted a topographic survey using auto level, stadia rod, and fiberglass tape. We also documented evidence of high water marks, such as trash lines where piles of woody debris were left suspended on channel banks, to use in the hydraulic roughness calculation.

I tied the surveyed cross sections into an adjacent vertical control monument on Dublin Blvd, or other *ad hoc* benchmarks and monuments documented by Krofta & Novotney (2003), and also established a new monument pin on the right overflow channel bank of each cross section. With a known vertical datum, the cross sections could then be overlayed on top of prior cross sections (Hudzik & Truitt, 2001; Krofta & Novotney, 2003; Tompkins, 2006; Butler & Nolan, 2007) and inspected for geomorphic change and evidence of incision. While every effort was made to precisely relocate the previous cross sections, some slight differences may persist due to the lack of extant permanent monuments.

I also conducted longitudinal surveys of selected reaches: the upstream section from the Gleason Dr culvert approaching the pedestrian bridge, and the downstream section from Dublin Blvd to Interstate 580. Dense willow growth in the channel, steep banks and deep water inhibited a long profile survey in the middle reach based on available resources, but local profiles were measured near cross sections D, E, and F to characterize channel slope at these locations. Profile surveys used auto level and stadia rod for differential leveling, with sighting distances measured

using the stadia intercept method, and relative heading angles used to derive channel distance with the law of cosines.

1D hydraulic model

In spring and summer 2022, I identified and surveyed high water marks under the Interstate 580 bridge south of the project reach. Using the known geometry, slope, and roughness of the concrete trapezoidal channel, I calculated the recent high flow using Manning's equation:

$$Q = V \cdot A = 1.486 \cdot A \cdot R^{2/3} \cdot S^{1/2} \ / \ n$$

where Q is the discharge (ft^3/s), V is the velocity (ft/s), R is the hydraulic radius (ft), A is the cross-sectional area (ft^2), S is the slope, and n is the roughness coefficient (Table 3). For each upstream cross section, I could then solve Manning's equation for the roughness coefficient, using the calculated discharge and the surveyed cross section geometry under the measured trash lines (Table 4). I observed trash lines at cross-sections B, D, E, and H, so I was able to back-calculate the channel roughness for these sections. For the sections without trash lines, I used adjacent values: cross section E roughness was assumed for cross section F, and cross section H roughness was assumed for cross section G. The average slope at each cross section was determined using the long profile distance and elevation change from the nearest adjacent upstream and downstream cross section.

Finally, I ran a one-dimensional (1D) steady state hydraulic model using the Hydrologic Engineering Center's River Analysis System (HEC-RAS) with a series of flows, ranging from the 2-year to 100-year flow (Table 2), to estimate conveyance (freeboard) under the current channel condition. Design discharges from BKF engineers were 650 cfs for the 2-year flow and 1200 cfs for the 5-year flow (Brian Kangas Foulk Engineers, 1999; as reported in Chan & Heard, 2006). I also used both the 100-year flow estimates from Alameda County (5200 cfs) and FEMA (4300 cfs) for modeling, along with reference flows, including the peak flow from the historic storm on 5 January 1982, the smaller recent storm that took place on 11 November 2022, and the flow derived from the Interstate 580 high water mark, which I inferred to date from October 2021.

The scope of the model was the reach from Gleason Drive to Interstate 580. I applied the normal depth assumption to determine the boundary conditions, using a slope of 0.10 as measured at both the Gleason Ave culvert (upstream) and the Interstate 580 culvert (downstream). I applied the back-calculated roughness coefficients to the channel and the design roughness values of n=0.12 to the floodplain. I assigned an assumed roughness of n=0.016 to the upstream Gleason Dr and downstream Interstate 580 concrete culverts.

LiDAR surveys

I acquired a high resolution (20 pulses/m^2, QL0) LiDAR dataset for eastern Alameda County dating from 2 July 2021 (NV5 Geospatial Corvallis, 2021) (Figure 12) in addition to a lower resolution LiDAR dataset from 25 June–2 July 2006, both published by the United States Geological Survey (USGS). Both surveys were in the summer when stream flows are relatively low, but the inundated low flow channel bottom is still obscured. The 2021 LiDAR dataset, with an associated digital elevation model (DEM) of 1-foot resolution, will provide the basis for future floodplain mapping and terrain modeling. Additionally, to compare the two datasets, I took spot ground elevations from both point clouds on a 3-foot grid and subtracted them, using inverse distance weighting to fill gap cells where pairs of points were not available, and masking out the low flow channel where data are unreliable due to inundation. The geoprocessing procedure is illustrated in Appendix A: Geospatial Models.

Results

Geomorphic surveys

Cross section survey results are reported in Figure 13. The longitudinal profile of the entire stream is illustrated in Figure 14 while the detailed longitudinal profile survey results are shown in Figure 15 (upper reach) and Figure 16 (lower reach).

In the upper reach, where the channel was re-rerouted into a meandering form and the original channel maintained as a secondary overflow, pool-riffle sequences occurred all along the channel, as captured in the longitudinal profile survey. Vegetation growth and accumulated debris in the channel have created complex channel form, with alternating zones of ponded water and zones of narrow, fast flow. My re-survey of cross section B suggests aggradation along the right bank, in an area currently occupied by a tangle of willows (Figure 17; Figure 18).

Likewise, the 2022 resurvey of cross section D, in the entrenched middle reach, indicates substantial overbank deposition and the buildup of natural levees in the period between the 2005/2006 and 2022 surveys, perhaps during the 2013 and 2017 storms which exceeded a 5-year recurrence interval (Figure 29). While flows of this magnitude appear to have inundated the floodplain and deposited sediment, such flows are relatively infrequent, with only four flows likely to have gone overbank since the project was completed in 2000 (in water years 2003, 2006, 2013, and 2016 based on flow recorded at nearby gauges; Figure 29). In many places in this middle reach the channel remains steep and simplified, lacking the alcoves, bank undercuts, and sequences of pool-riffle bedforms that are necessary for diverse aquatic habitat.

Farther downstream in the middle reach at cross section E, the 2022 survey shows increases in floodplain elevation (Figure 19). This increase may reflect overbank deposition but may also be attributable to a cross section misalignment due to poorly defined monuments. The geometry of cross section F is nearly identical to prior surveys; changes in elevation indicate aggradation but may also be an artifact of the higher resolution of the 2022 survey.

In the lower reach with the lower-capacity 2-year flow channel, the 2022 survey of cross section G suggests overbank deposition and the formation of a natural levee on the left bank. At the farthest downstream cross section H, apparent deposition within the low flow channel has led to the formation of complex microtopography (Figure 20). Cottonwood seedling recruitment, debris deposition among wetlands plants, step-pool topography, and secondary cutoff channel development were all observed at this location.

Hydraulic model

Preliminary outputs from the 1D hydraulic model are shown in Figure 21 (longitudinal profile) and Figure 22 (by cross section). Floodplain activation frequency varies by cross section and generally increases farther downstream. Bankfull capacity is approximately the 2-year flow for cross sections G and H, the 5-year flow for cross-sections B, E, and F, and an intermediate flow for cross section G. Overbank velocities for the 5-year storm are modeled at around 1 ft/s on cross sections G and H, while corresponding in-channel velocities are in the range of 6 to 8 ft/s.

100-year freeboard estimates range from 1.7 to 5.4 feet (Table 5; Figure 23). These are conservative freeboard estimates because the very high design roughness of n=0.12 is applied to the overbank floodplain, and the higher 100-year flow estimate from Alameda County (5,200 cfs) is used. As expected, the freeboard for the flood control channel is lowest at cross section E, where the channel width was constrained by the presence of an old growth oak tree on the upper left bank. In-channel velocities at this location are the greatest, exceeding 10 ft/s in the 5-year flood.

Using rating curves of depth versus discharge output from HEC-RAS (Figure 24), bankfull discharge was derived for each cross section (Table 6). Approximate recurrence intervals were then determined based on power function interpolation of the published Tassajara Creek 2-year, 5-year, and 100-year flows, because the creek does not have a long term gauge (Figure 25). Bankfull discharge ranges from as low as 563.5 cfs in cross section H, a 1.4-year flow, to as high as 1727.6 cfs in cross section B, an 8.7-year flow (Table 6). Bankfull discharge is less than the BKF design 2-year flow for the two lowest cross sections (cross sections G and H) and exceeds the design 5-year flow for all the other cross sections.

LiDAR data comparison

Differencing of the 2006 and 2021 LiDAR floodplain data, illustrated in Figure 26, suggests substantial changes in the upper reach that align with observations from the cross-section overlays. Overbank aggradation is apparent on either side of the low flow channel between the Gleason Dr culvert and the Central Pkwy crossing, as well as on the downstream end of the promontory between cross sections B and D. The difference in elevation is as high as 4 ft on cross section B, 3 ft at the promontory, and 2.5 ft on cross section D. Negative elevation changes (soil loss) are detected at the known scour pools on the distal side of the promontory, and at a location on the side of the promontory where a buckeye tree uprooted and slid. Some of the detected changes, such as the apparent decrease in elevation at the scour pools, may be due to the increased resolution of the second LiDAR survey relative to the first. However, for others, such as the erosion near the buckeye, evidence in the field is consistent with the LiDAR results.

Discussion

Assessed against its primary goal of curbing incision, results are strongly positive for the Lower Tassajara Creek project. So far, the project has been tested by four storms that exceeded the 5-year level, including the >15-year storm in water year 2006, and substantial additional channel incision has not been documented at any of the cross sections. The following section dives deeper into the components of project performance relevant to floodplain reconnection.

Observed overbank deposition

Both the LiDAR comparison and the cross-section overlays revealed apparent depositional landforms that appeared between 2006 and 2021. These areas are concentrated in the upper reach from Gleason Dr to Central Pkwy, including at cross sections B and D, and are consistent between the two analyses. Zones of increased elevation tend to extend in the longitudinal direction, including downstream of existing landforms (e.g., the depositions below the promontory) and vegetation (e.g., at the coyote brush on the floodplain near cross section D) or among dense willows (as observed on the right bank at cross section B). The longitudinal forms on the floodplain near cross section D are among the most visually striking; they are made up largely of sand with a consistently fine texture (Figure 28). I excavated a hole at cross section B and observed coarser sand at depths of 2 feet below the surface, with finer sand at the surface (Figure 27).

Flow history data can be used to determine the storms that may have contributed to this potential overbank deposition. While there was no recording gauge on Tassajara Creek prior to

2021,[3] we can synthesize a flow record from the continuous flow record for San Ramon Creek at Bollinger Canyon (USGS gauge 11182500), 12 km west of Tassajara Creek. Based on 70 years of peak flow history at this gauge, four water years between 2000 and 2022 had flows exceeding the 5-year recurrence interval (2003, 2006, 2013, 2017) while five additional years had flows exceeding the 2-year recurrence interval (2000, 2004, 2011, 2019, 2022) (Figure 29). Assuming similar *relative* flow magnitudes for Tassajara Creek, in the time since last survey, overbank flows may have occurred in 2013 and 2017 for the middle reach (with approximately 5-year capacity low flow channel) and additionally in 2011, 2019, and 2022 for the lower reach (with approximately 2-year capacity low flow channel). The actual result will vary as channel capacities are not exactly the 2-year or 5-year flow, and flows may longitudinally bypass natural levees to overbank easier than indicated by cross-section-based model.

Shallow slopes and fine sediment deposition

In a reversal of the active incision documented in Tassajara Creek in the late 1990s, my 2022 cross section resurveys indicate deposition in many parts of the reach. A depositional trend should not be surprising given the larger context: the study reach is located at the transition from the mountainous terrain along the south side of Mount Diablo to the alluvial plain of the Amador-Livermore Valley, which creates a local base level control for the Lower Tassajara Creek and places it in a natural depositional zone. Its location is at the toe of the foothill slopes, where the stream formerly opened out into willow thicket and tule marsh (Stanford et al., 2013), flowing into a historic sediment sink (Bigelow et al., 2012, p. 22). Just as ranchers once reported the *Tasajero*'s banks overflowing and fine silts depositing over the landscape (Stanford et al., 2013), on-site observations confirmed the presence of fine silts in the channel and overbank sediment deposition. In most parts of the project reaches, stream channel sediment is dominated by fine silt and sand with occasional fine gravels. Most large cobbles and boulders observed were introduced in the channel rehabilitation for grade control or are broken remnants of pre-restoration concrete structures.

The coarse profile of the reach, taken by connecting the cross-section thalwegs, reveals slopes ranging from 1% at the upper end to as low as 0.3% in the lower middle reach. Detailed longitudinal profile surveys confirm that locally, even shallower slopes and positive slopes are common. In-stream sediment deposition and debris buildup creates stagnant pools that cease to flow entirely at baseflow. For a multi-benefit flood control and ecological restoration project,

[3] The USGS gauge for Tassajara Creek (11176300) has data available for 1915–1930 and again for 1979–1983, but this is not enough to conduct flow frequency calculations. The new gauge reporting since 2021 ("Tassajara Creek Below I-580") is operated by Zone 7 Water Agency.

sediment deposition is valuable ecologically, but also problematic when it comes to flood conveyance. The reduction of transport capacity due to sediment buildup is a frequent challenge for floodplain reconnection projects in depositional zones (Haltiner & Beeman, 2003). However, where excess conveyance capacity allows, the trapping of sediment in the stream reach may help to prevent the filling of more constrained channels downstream. Therefore, the site may present an opportunity to act as a strategic sediment sink.

Ongoing entrenched conditions in middle reach

The middle reach continues to be entrenched and lacks frequent overbank flows, an observation first reported by Tompkins (2006). While the channel rehabilitation project appears to have halted ongoing incision and returned the lower creek system to a depositional condition, channel capacity along this section remains at or above the 5-year flow as constructed.

Field evidence of persistent entrenched conditions in the middle reach presents an opportunity for intervention. Low-cost woody debris placement and "beaver dam analogues" are among the solutions increasingly proposed for process-based restoration of river-floodplain-meadow ecosystems (Beechie et al., 2010). While right-of-way width and flood conveyance capacity constraints limit the applicability in urban flood control settings, preliminary hydraulic model results indicated that parts of the Tassajara Creek channel have capacity well exceeding the 100-year flood, even with a floodplain highly roughened by vegetation. The notable exception is the location near cross section E, and another farther downstream, where the overflow channel was narrowed to protect old growth valley oaks on the upper bank. Future research, after further developing the hydraulic model, should test scenarios for strategic woody debris placement (Addy & Wilkinson, 2019) in the incised middle reach.

Hydraulic model limitations

The one-dimensional hydraulic model is a broad simplification of the stream corridor system. While it may provide a sufficiently realistic simplification of in-channel conditions to model water surface elevations at each cross section, the complexity of overbank floodplain flow is not well-represented. In reality, overbank flows would follow a complex network of nascent channels and swales created by longitudinal earthen forms and would encounter varying resistance from the mosaic of riparian vegetation. The resulting variations in flow direction, velocity, and roughness would be better represented by a spatially explicit two-dimensional hydraulic model. Additionally, the one-dimensional model calculates slope based on the overall change in elevation from one cross section thalweg to the next. This may be relevant for high

flows, but at low flow, subtleties in channel bedform produce highly variable and at times extremely shallow slopes locally. These local slopes are not effectively accounted for in the hydraulic model.

Restoration goals and reference sites

The downstream reach evinced the strongest evidence of successful floodplain reconnection. The downstream reach coincides with the part of the site that historically ran through a shallow-sloped alkali wet meadow ecosystem, just prior to meeting up with the freshwater marsh (*tulare*) and willow thicket (*sausal*). This was the shallow part of the creek that 19th-century rancheros reported to frequently flood and deposit overbank sediment. This portion of the project section benefits from a lower-capacity low flow channel, making it more possible to continue supporting historically-analogous depositional conditions and freshwater wetland ecosystems, at least locally. Bulrush and sedges observed in the low-flow channel today would have been characteristic of the pre-development freshwater marsh ecology.

While historical ecology provides a valuable lens for evaluating site conditions and expected geomorphic outcomes, full restoration of these historical conditions is limited in the highly constrained urban environment, and is subject to additional considerations (Van Dam, 2013). The dense willows that have established along parts of the Tassajara Creek project may be historically appropriate given the documentation of willow thicket (*sausal*) in this area, but as an element of public recreational space, they prevent visual line-of-sight across the creek. Willows are planted as reliable and quick-growing bank stabilization that reduces the risk of channel blowout in a storm shortly after construction. In theory, the "awkward teenage years" of a low, dense understory or willow thicket may eventually give way to a mature, higher riparian canopy (e.g. cottonwood or alder) that both allows line-of-sight and creates less hydraulic resistance. Ecological disturbance, however, favors early-successional species and prevents the development of climax communities (Suding et al., 2004). Restoration sites in urban areas are likely to remain in a suspended state of degradation, limiting the possibility of development into mature forest.

The historically documented riparian ecosystem existed within a vastly different overall catchment hydrology. As with so many places where multi-channel stream-meadow systems have been converted into single-threaded channels (Cluer & Thorne, 2014, p. 136), the extent of regional hydrologic modification is such that "intact" reference sites are likely nonexistent. Before the Amador-Livermore Valley basin was channelized and exploited for a water supply and storage, water tables were high enough to create free-flowing artesian wells on the alluvial fan.

Tassajara Creek, lined with oaks and sycamores, passed through seasonally saturated alkali wet meadow. Today's post-restoration Tassajara Creek corridor remains confined to a relatively narrow belt of activated floodplain compared to the connected wet meadow hydrology of the prior system. A relevant contemporary reference site for the rehabilitated compound channel might be the confined bedrock canyons of upper Alameda Creek, which support willow, sycamore, cottonwood, and oak woodlands on narrow adjacent floodplains.

Because Lower Tassajara Creek is an urban stream project promising recreational amenities in addition to ecological and flood control benefits, project success must be evaluated under social criteria as well. Performance regarding the three dimensions of social connectivity (longitudinal, lateral, and vertical; Kondolf & Pinto, 2017) varies along the stream corridor. The upper reach near Emerald Glen Park not only experiences the most foot traffic along the adjacent trails and service roads, but also allows pedestrian access to the stream itself at times of low flow, the only instance of vertical connectivity on the site. No other locations permit direct access to the creek, and stepping off the path into the floodplain is prohibited throughout, even in the dry season. Lateral connectivity across the corridor is inhibited by low visibility from the dense willow thickets. Furthermore, the entire lower reach does not even permit pedestrian access on the longitudinal service roads. To improve the creek corridor's social benefits, opportunities to increase direct pedestrian access to the channel, floodplain, and upper banks merit further exploration.

Conclusions

The results of this preliminary study suggest overall positive geomorphic outcomes for the Lower Tassajara Creek restoration project, with some notable exceptions. The site has been tested by four 5-year storms and channel incision is not evident; on the contrary, the low flow channel environment appears to be largely depositional, and observed depositional landforms on the floodplain indicates some level of active floodplain connection. The middle reach, however, continues to suffer from entrenched conditions, with steep banks and fewer well-developed bedforms. Looking to its history as a distributary into a freshwater wetland may help to suggest future interventions, such as woody debris placement in the low flow channel, that could improve floodplain reconnection for these segments. Such an intervention would be limited by overflow channel capacity, and likely not possible in some locations, but Tassajara Creek's unusually wide right-of-way may make this possible, warranting future research.

References

Addy, S., & Wilkinson, M. E. (2019). Representing natural and artificial in-channel large wood in numerical hydraulic and hydrological models. *WIREs Water*, *6*(6), e1389. https://doi.org/10.1002/wat2.1389

Beechie, T. J., Sear, D. A., Olden, J. D., Pess, G. R., Buffington, J. M., Moir, H., Roni, P., & Pollock, M. M. (2010). Process-based Principles for Restoring River Ecosystems. *BioScience*, *60*(3), 209–222. https://doi.org/10.1525/bio.2010.60.3.7

Bigelow, P. E., Pearce, L., Benda, K., Andras, K., McKee, L., & Kass, J. (2012). *Geospatial Terrain Analysis of Sediment Sources within the Arroyo Mocho Watershed*. Prepared for Zone 7 Water Agency, Livermore, CA. http://www.netmaptools.org/Pages/Arroyo_Mocho_erosion_analysis.pdf

Bowles, F., Clarke, S., Eardley, B., Jeffries, R., & Stone, P. (2021). The Stage Zero approach – lessons from North America on restoring river, wetland and floodplain habitats. *Conservation Land Management*, *19*(4), 21–28.

Bravard, J.-P., Kondolf, G. M., & Piegay, H. (1999). Environmental and Societal Effects of Channel Incision and Remedial Strategies. In S. E. Darby & Simon (Eds.), *Incised River Channels* (p. 21).

Brian Kangas Foulk Engineers. (1999). *Improvement Plans for Tassajara Creek Restoration*.

Brookes, A. (1989). Alternative Channelization Procedures *. In J. A. Gore & G. E. Petts (Eds.), *Alternatives in Regulated River Management* (1st ed., pp. 139–162). CRC Press. https://doi.org/10.1201/9781351069595-5

Brookes, A., Baker, J., & Redmond, C. (1996). Floodplain Restoration and Riparian Zone Management. In A. Brookes & F. D. Shields (Eds.), *River Channel Restoration: Guiding Principles for Sustainable Projects* (p. 15).

Butler, N. L., & Nolan, L. (2007). *Evolution of a Compound Channel: Tassajara Creek, Dublin, California*. RiverLab, UC Berkeley. https://escholarship.org/uc/item/6ws5915v

Chan, A., & Heard, S. K. (2006). *The perfect storm: Flow through a restored compound channel, Tassajara Creek, Dublin, CA*. RiverLab, UC Berkeley. https://escholarship.org/uc/item/1hp742bt

Ciotti, D. C., Mckee, J., Pope, K. L., Kondolf, G. M., & Pollock, M. M. (2021). Design Criteria for Process-Based Restoration of Fluvial Systems. *BioScience*, *71*(8), 831–845. https://doi.org/10.1093/biosci/biab065

Cluer, B., & Thorne, C. (2014). A Stream Evolution Model Integrating Habitat and Ecosystem Benefits. *River Research and Applications*, *30*(2), 135–154. https://doi.org/10.1002/rra.2631

Dunne, T., & Leopold, L. B. (1978). *Water in environmental planning*. W. H. Freeman.

Groffman, P. M., Bain, D. J., Band, L. E., Belt, K. T., Brush, G. S., Grove, J. M., Pouyat, R. V., Yesilonis, I. C., & Zipperer, W. C. (2003). Down by the riverside: Urban riparian ecology. *Frontiers in Ecology and the Environment*, *1*(6), 315–321. https://doi.org/10.1890/1540-9295(2003)001[0315:DBTRUR]2.0.CO;2

Haltiner, J. P., & Beeman, C. (2003). Restoring floodplain and channel functions to incised and leveed stream systems. In P. M. Faber (Ed.), *California Riparian Systems: Processes and Floodplain Management, Ecology, and Restoration* (pp. 210–223). 2001 Riparian Habitat and Floodplains Conference Proceedings, Riparian Habitat Joint Venture, Sacramento, CA.

Haltiner, J. P., Kondolf, G. M., & Williams, P. B. (1996). Restoration Approaches in California. In A. Brookes & F. D. Shields (Eds.), *River channel restoration: Guiding principles for sustainable projects*. J. Wiley.

Hoffmann, C. F., & Whitney, J. D. (1873). *Composite: Map Of The Region Adjacent To The Bay Of San Francisco.* [Map]. Geological Survey of California. David Rumsey Historical Map Collection. https://www.davidrumsey.com/luna/servlet/detail/RUMSEY~8~1~203546~3001695:Composite--Map-Of-The-Region-Adjace

Hudzik, C. M., & Truitt, J. (2001). *Characterization of channel morphology in the Tassajara Creek restoration project area: Documentation of post-project change and recommendations for a monitoring plan*. Water Resources Collection & Archives, UC Riverside.

Junk, W., Bayley, P. B., & Sparks, R. E. (1989). The Flood Pulse Concept in River-Floodplain Systems. *Canadian Journal of Fisheries and Aquatic Sciences*, *106*.

Knudsen, K. L., Sowers, J. M., Witter, R. C., Wentworth, C. M., & Helley, E. J. (2000). *Preliminary Maps of Quaternary Deposits and Liquefaction Susceptibilty Nine-County San Francisco Bay Region, California: A Digital Database* (USGS Open-File Report 00-444). US Geological Survey. https://pubs.usgs.gov/of/2000/of00-444/

Kondolf, G. M., & Pinto, P. J. (2017). The social connectivity of urban rivers. *Geomorphology*, *277*, 182–196. https://doi.org/10.1016/j.geomorph.2016.09.028

Kondolf, G. M., Podolak, K., & Grantham, T. E. (2013). Restoring mediterranean-climate rivers. *Hydrobiologia*, *719*(1), 527–545. https://doi.org/10.1007/s10750-012-1363-y

Krofta, C., & Novotney, M. (2003). *Looking forward, looking back: Monitoring the Tassajara Creek Restoration Project*. RiverLab, UC Berkeley. https://escholarship.org/uc/item/3ft991xc

Lane, B. (2006, August 11). Tassajara: A melodious name with a not-so-melodious meaning [Originally published in the *Danville Express* column "Presenting the Past"]. *Museum of the San Ramon Valley*. https://museumsrv.org/post-1483/

Ludington, S., Moring, B. C., Miller, R. P., Stone, P. A., Bookstrom, A. A., Bedford, D. R., Evans, J. G., Haxel, G. A., Nutt, C. J., Flyn, C. S., & Hopkins, M. J. (2005). *Preliminary Integrated Geologic Map Databases of the United States: The Western States: California, Nevada, Arizona, Washington, Idaho, Utah* (USGS Open-File Report 2005-1305). US Geological Survey. https://pubs.usgs.gov/of/2005/1305/#CA

Middleton, B. (2002). The flood pulse concept in wetland restoration. *Flood Pulsing in Wetlands: …*. https://www.academia.edu/12387186/The_flood_pulse_concept_in_wetland_restoration

NV5 Geospatial Corvallis. (2021). *USGS 3DEP Alameda County, California Lidar Technical Data Report* (p. 70). US Geological Survey. https://prd-tnm.s3.amazonaws.com/StagedProducts/Elevation/metadata/CA_AlamedaCounty_2021_B21/CA_AlamedaCo_3_2021/reports/Alameda_Technical_Data_Report_Final_Signed.pdf

Oakland Museum of California. (2008). *Guide to San Francisco Bay Area Creeks*. http://explore.museumca.org/creeks/index.html

Pollock, M. M., Beechie, T. J., Wheaton, J. M., Jordan, C. E., Bouwes, N., Weber, N., & Volk, C. (2014). Using Beaver Dams to Restore Incised Stream Ecosystems. *BioScience*, *64*(4), 279–290. https://doi.org/10.1093/biosci/biu036

Schumm, S. A. (1999). Causes and Controls of Channel Incision. In S. E. Darby & A. Simon (Eds.), *Incised River Channels* (pp. 19–33).

Schumm, S. A., Harvey, M. D., & Watson, C. C. (1984). *Incised channels: Morphology, dynamics, and control*. Water Resources Publications. https://scholar.google.com/scholar_lookup?title=Incised+channels%3A+morphology%2C+dynamics%2C+and+control&author=Schumm%2C+Stanley+A.&publication_year=1984

Serra-Llobet, A., Kondolf, G. M., Magdaleno, F., & Keenan-Jones, D. (2022). Flood diversions and bypasses: Benefits and challenges. *WIREs Water*, *9*(1), e1562. https://doi.org/10.1002/wat2.1562

Simon, A., & Hupp, C. R. (1986). Channel evolution in modified Tennessee channels. *Proceedings of the Fourth Federal Interagency Sedimentation Conference March 24-27, 1986, Las Vegas, Nevada*, *2*.

Stanford, B., Grossinger, R. M., Beagle, J., Askevold, R. A., Leidy, R. A., Beller, E. E., Salomon, M., Striplen, C. J., & Whipple, A. (2013). *Alameda Creek Watershed Historical Ecology Study*. San Francisco Estuary Institute. https://www.sfei.org/sites/default/files/biblio_files/AlamedaCreekHistoricalEcologyStudy_SFEI_2013_highres.pdf

Stella, J. C., Rodríguez-González, P. M., Dufour, S., & Bendix, J. (2013). Riparian vegetation research in Mediterranean-climate regions: Common patterns, ecological processes, and considerations for management. *Hydrobiologia*, *719*(1), 291–315. https://doi.org/10.1007/s10750-012-1304-9

Suding, K. N., Gross, K. L., & Houseman, G. R. (2004). Alternative states and positive feedbacks in restoration ecology. *Trends in Ecology & Evolution*, *19*(1), 46–53. https://doi.org/10.1016/j.tree.2003.10.005

Thompson & West. (1878). *Map number seven (Alameda County farm map)* [Map]. Thompson & West. David Rumsey Historical Map Collection. https://www.davidrumsey.com/luna/servlet/detail/RUMSEY~8~1~21371~620073:Alameda-Co--7-

Tompkins, M. R. (2006). Floodplain connectivity and river corridor complexity: Implications for river restoration and planning for floodplain management [Ph.D., University of California, Berkeley]. In *ProQuest Dissertations and Theses*. http://search.proquest.com/pqdtlocal1005845/docview/305364761/abstract/7591A7251FA841C0PQ/1

Tompkins, M. R., & Kondolf, G. M. (2007). Systematic Postproject Appraisals to Maximize Lessons Learned from River Restoration Projects: Case Study of Compound Channel Restoration Projects in Northern California. *Restoration Ecology*, *15*(3), 524–537. https://doi.org/10.1111/j.1526-100X.2007.00248.x

Trinh, M., & Percelay, J. (2008). *Tassajara Creek restoration project: Continued riparian habitat monitoring*. RiverLab, UC Berkeley. https://escholarship.org/uc/item/3c76c585

Unruh, J. R., Dumitru, T. A., & Sawyer, T. L. (2007). Coupling of early Tertiary extension in the Great Valley forearc basin with blueschist exhumation in the underlying Franciscan accretionary wedge at Mount Diablo, California. *Geological Society of America Bulletin*, *119*(11–12), 1347–1367. https://doi.org/10.1130/B26057.1

Van Dam, K. Juliann. (2013). Same time, different place: Deriving reference metrics for riparian vegetation from contemporary analog reference sites. In *Same time, different place: Deriving reference metrics for riparian vegetation from contemporary analog reference sites*. Professional paper (Master of Forestry)–University of California, Berkeley, Spring 2013.

Walsh, C. J., Roy, A. H., Feminella, J. W., Cottingham, P. D., Groffman, P. M., & Morgan, R. P. (2005). The urban stream syndrome: Current knowledge and the search for a cure. *Journal of the North American Benthological Society*, *24*(3), 706–723. https://doi.org/10.1899/04-028.1

Walter, R. C., & Merritts, D. J. (2008). Natural Streams and the Legacy of Water-Powered Mills. *Science*, *319*(5861), 299–304. https://doi.org/10.1126/science.1151716

Williams, P. B., Andrews, E., Opperman, J. J., Bozkurt, S., & Moyle, P. B. (2009). Quantifying Activated Floodplains on a Lowland Regulated River: Its Application to Floodplain Restoration in the Sacramento Valley. *San Francisco Estuary and Watershed Science*, *7*(1). https://doi.org/10.15447/sfews.2009v7iss1art4

Wolman, M. G. (1967). A Cycle of Sedimentation and Erosion in Urban River Channels. *Geografiska Annaler: Series A, Physical Geography*, *49*(2–4), 385–395. https://doi.org/10.1080/04353676.1967.11879766

Tables

Table 1. Summary of cross section stations

	Approx. station on project control line	Channel distance from upstream	Roughness from Chan & Heard	Design Roughness overbank	Design roughness channel	Long profile slope
Gleason	113+00	0	NA	NA	0.0160	0.010
XS B	108+00	500	0.0865	0.1200	0.0400	0.012
XS D	102+00	1100	0.0368	0.1200	0.0400	0.005
XS E	93+00	2000	0.0685	0.1200	0.0400	0.003
XS F	88+00	2500	0.0705	0.1200	0.0400	0.003
XS G	82+00	3100	0.0520	0.1200	0.0400	0.003
XS H	76+00	3700	0.0380	0.1200	0.0400	0.003
I-580	69+00	4400	0.0110	NA	0.0160	0.010

Table 2. HEC-RAS model specifications

Steady Flow Profiles

Published peak flows:	Q2	650 cfs
	Q5	1,200
	Q100 FEMA	4,300
	Q100 Alameda Co.	5,200
Reference flows:	I-580 HWM	559.83
	5 Jan 1982	2,280
	11 Nov 2022	105.2

Table 3. Hydraulic calculations for derived peak flow at I-580

A	xs area under hwm	46.08	ft^2 / s
P	wetted perim under hwm	30.80	ft
R	hydraulic radius	1.50	ft
S	water surface slope	0.010	ft / ft
n	Manning's roughness	0.016	$m^{1/3}$ / s
Q	discharge	559.83	ft^3 / s

Table 4. Hydraulic calculations for cross sections under high water mark

		B	D	E	F	G	H	
	HWM elevation	355.72	353.36	351.76			343.20	ft NGVD29
Q	discharge	559.83	559.83	559.83			559.83	ft^3 / s
A	cross-sectional area	60.32	59.82	86.97	no HWM; use same as E	no HWM; use same as H	113.29	ft^2 / s
P	wetted perimeter	26.70	21.83	27.33			54.04	ft
R	hydraulic radius	2.26	2.74	3.18			2.10	ft
S	water surface slope	0.012	0.005	0.003			0.003	ft / ft
n_{LF}	roughness, low flow	0.030	0.022	0.028	0.028	0.028	0.028	$m^{1/3}$ / s
n_{FP}	roughness, floodplain	0.120	0.120	0.120	0.120	0.120	0.120	$m^{1/3}$ / s

Table 5. 100-year flow freeboard

(see also Figure 23)	B	D	E	F	G	H	
thalweg elevation	351.6	347.9	344.3	343.2	341.6	339.4	ft NGVD29
bank elevation	370.05	364.88	359.95	356.01	353.96	352.44	ft NGVD29
Q100 water surface	364.7	363.2	358.3	354.2	350.7	349.6	ft NGVD29
Q100 water depth	-13.1	-15.3	-13.9	-11.1	-9.1	-10.3	ft
Q100 freeboard	5.4	1.7	1.7	1.8	3.3	2.8	ft

Table 6. Bankfull discharge estimates

	B	D	E	F	G	H	
rating curve: H =	$0.16\ Q^{0.53}$	$0.42\ Q^{0.44}$	$0.44\ Q^{0.42}$	$0.53\ Q^{0.38}$	$0.48\ Q^{0.34}$	$0.26\ Q^{0.43}$	
(Figure 24)							
thalweg elevation	351.6	347.9	344.3	343.2	341.6	339.4	ft NGVD29
left bank elevation	361.89	356.38	352.87	350.23	346.44	344.4	ft NGVD29
right bank elevation	359.08	357.44	352.73	350.28	346.27	343.16	ft NGVD29
bankfull depth	7.5	8.5	8.4	7.0	4.7	3.8	ft
bankfull discharge	1479.2	1137.1	1310.9	1344.0	781.6	563.5	cfs
rating curve: Q =	$480\ P^{-0.521}$						
(Figure 25)							
probability	0.12	0.19	0.15	0.14	0.39	0.74	
recurrence Interval	8.65	5.22	6.86	7.20	2.54	1.36	y

Figures

Figure 1. Map of study site, catchment area, and regional river network

(original; catchment area calculated from USGS NHD+HR)

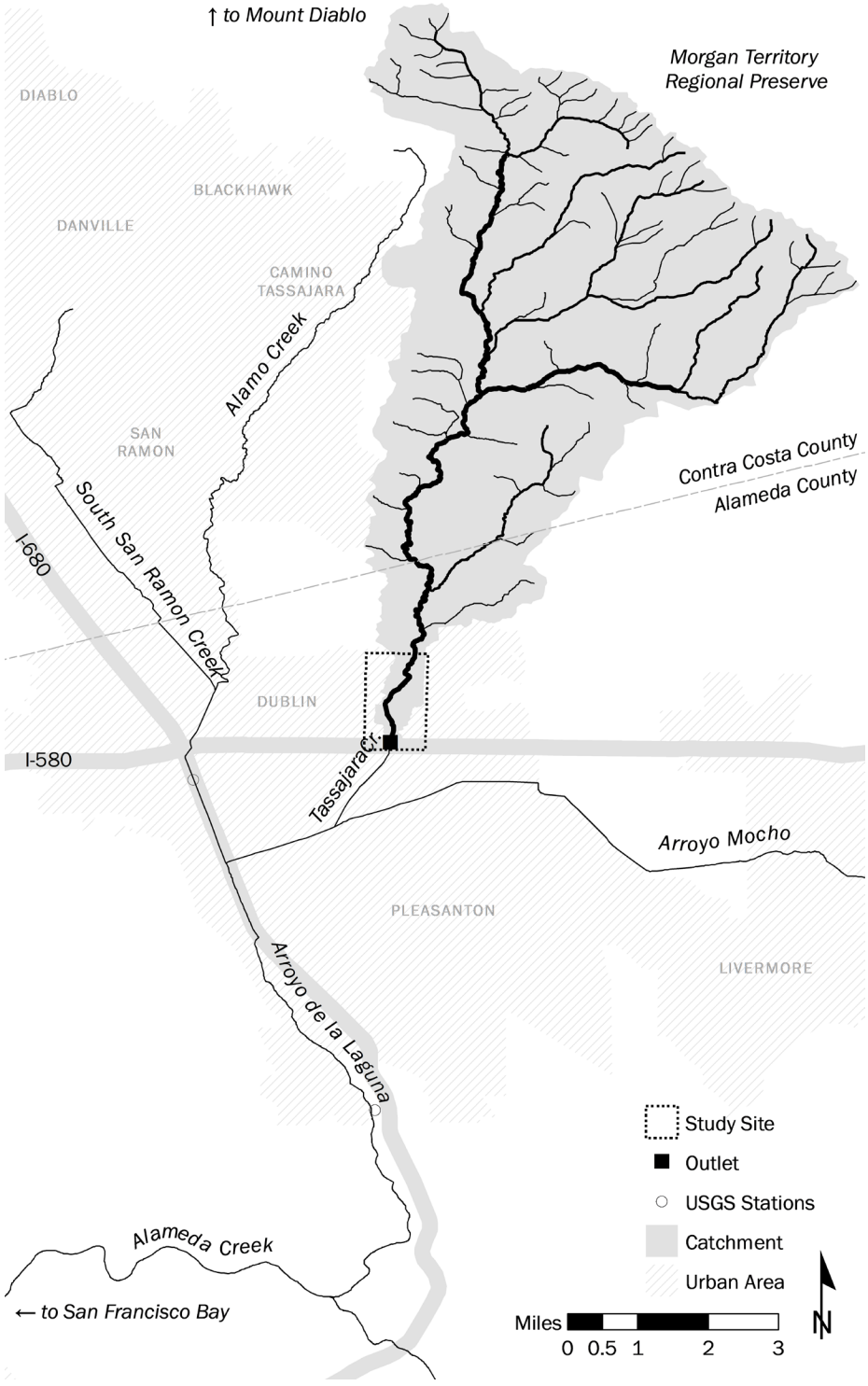

Figure 2. Aerial imagery: 1992, 2002, 2020

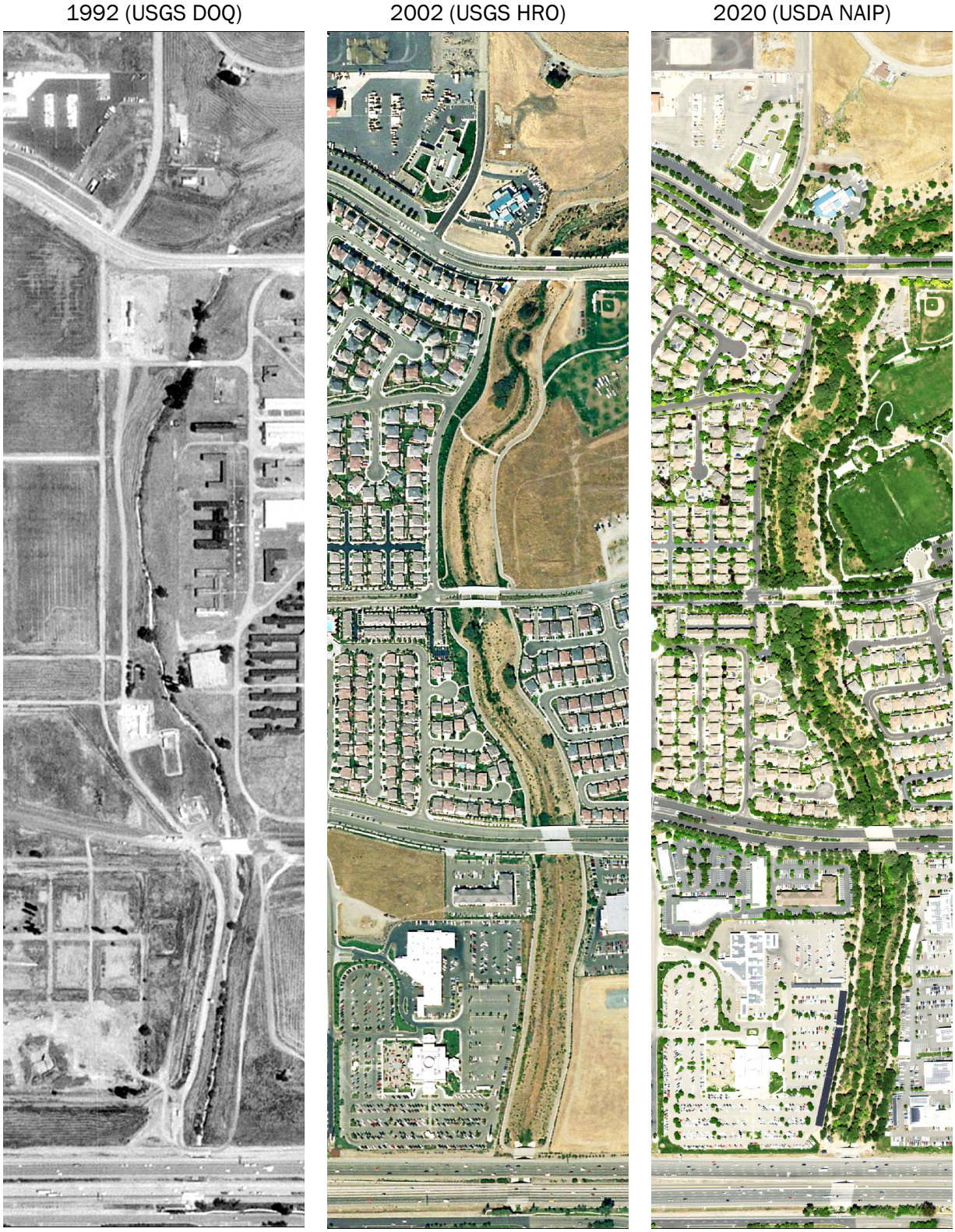

Figure 3. Pre-project photos showing incised conditions

Figure 4. Post-restoration photo time series south of Gleason: 2001, c.2007, 2021

Figure 5. Lower Tassajara Creek project reaches and cross section locations

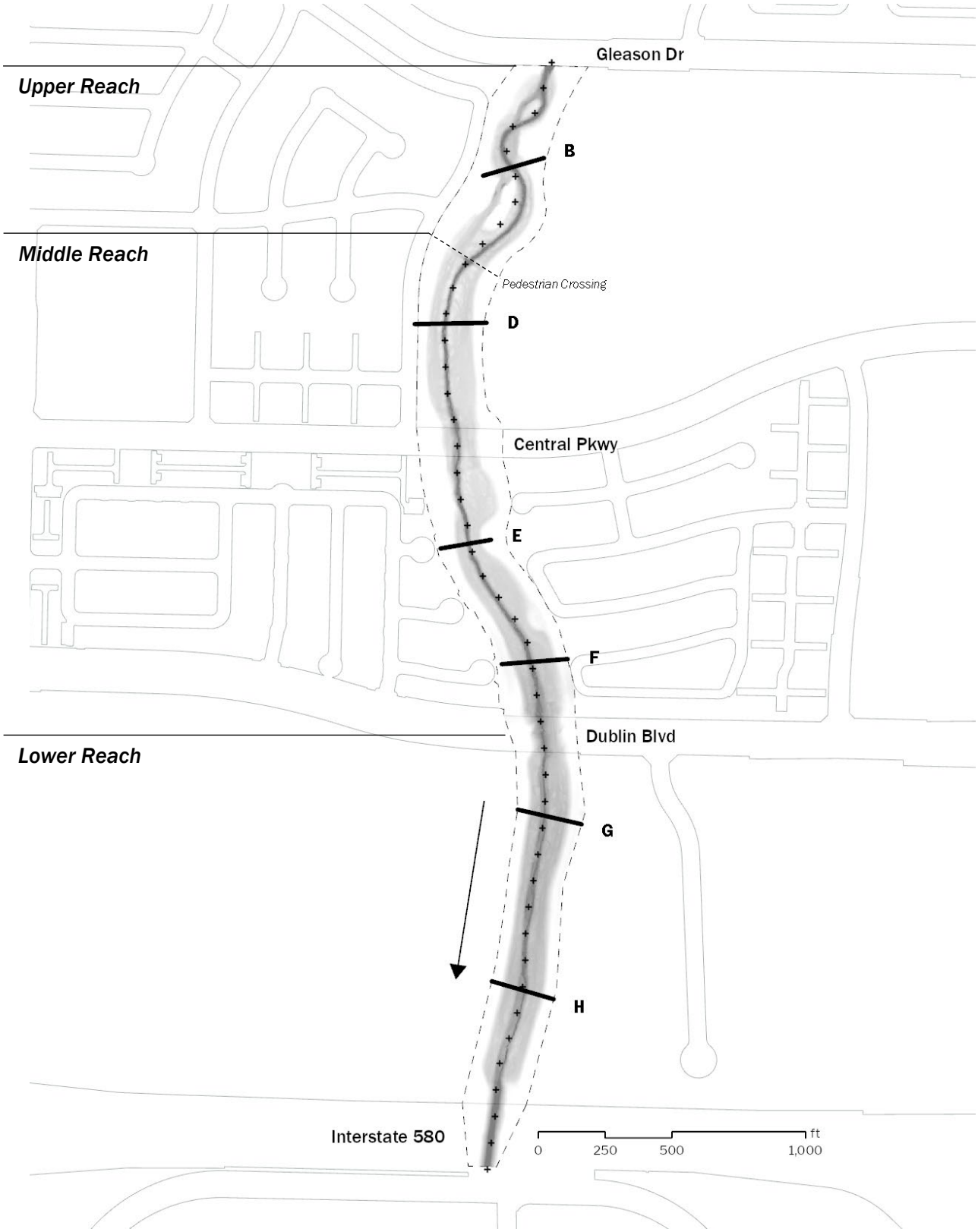

Figure 6. Map showing historical hydrology and ecology of Amador Valley

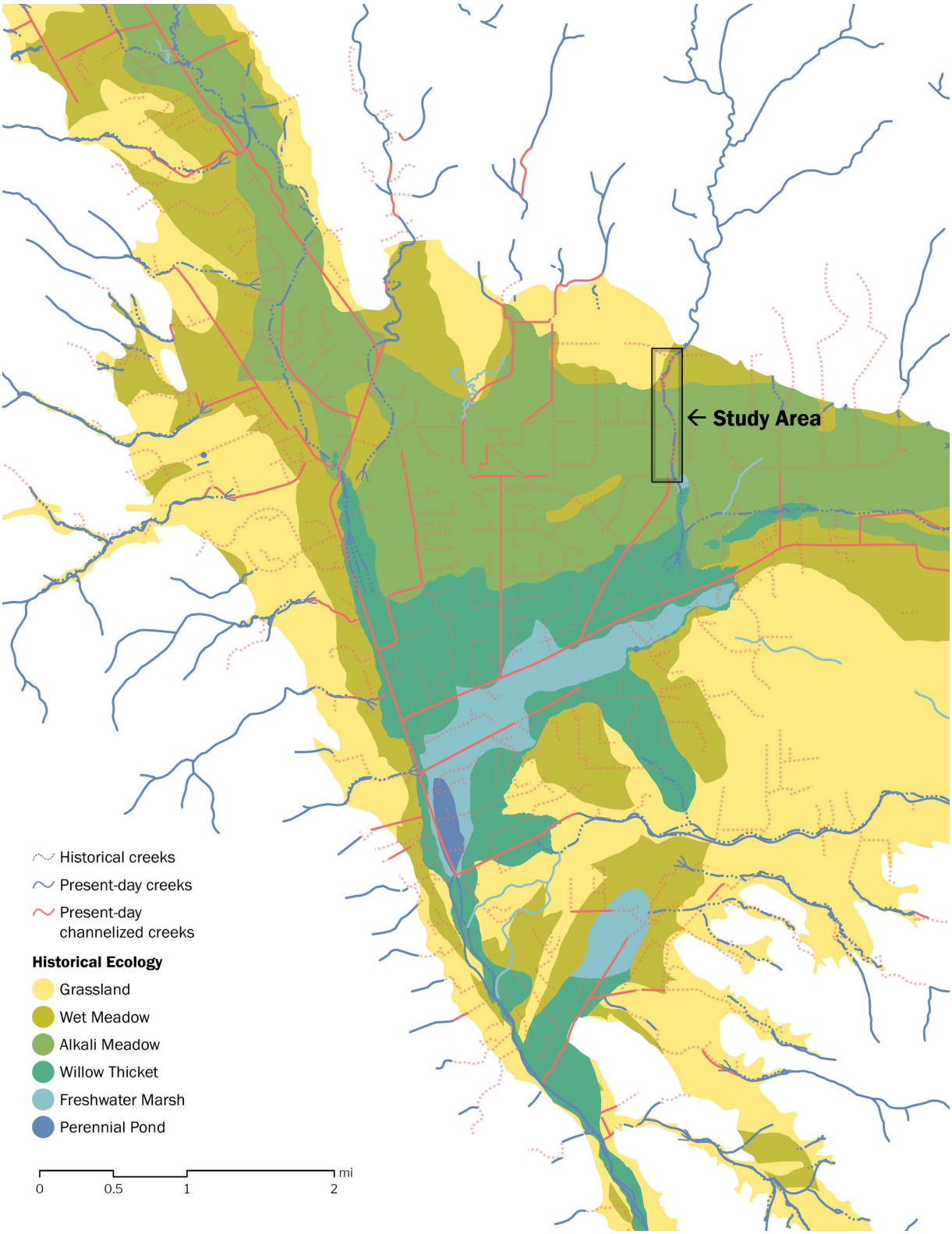

Data sources: SFEI (Stanford et al., 2013), Oakland Museum of California (2008)

Figure 7. Surficial geology (left) and hydrologic soil group (right), Tassajara Creek basin

(a) Quaternary and bedrock geology

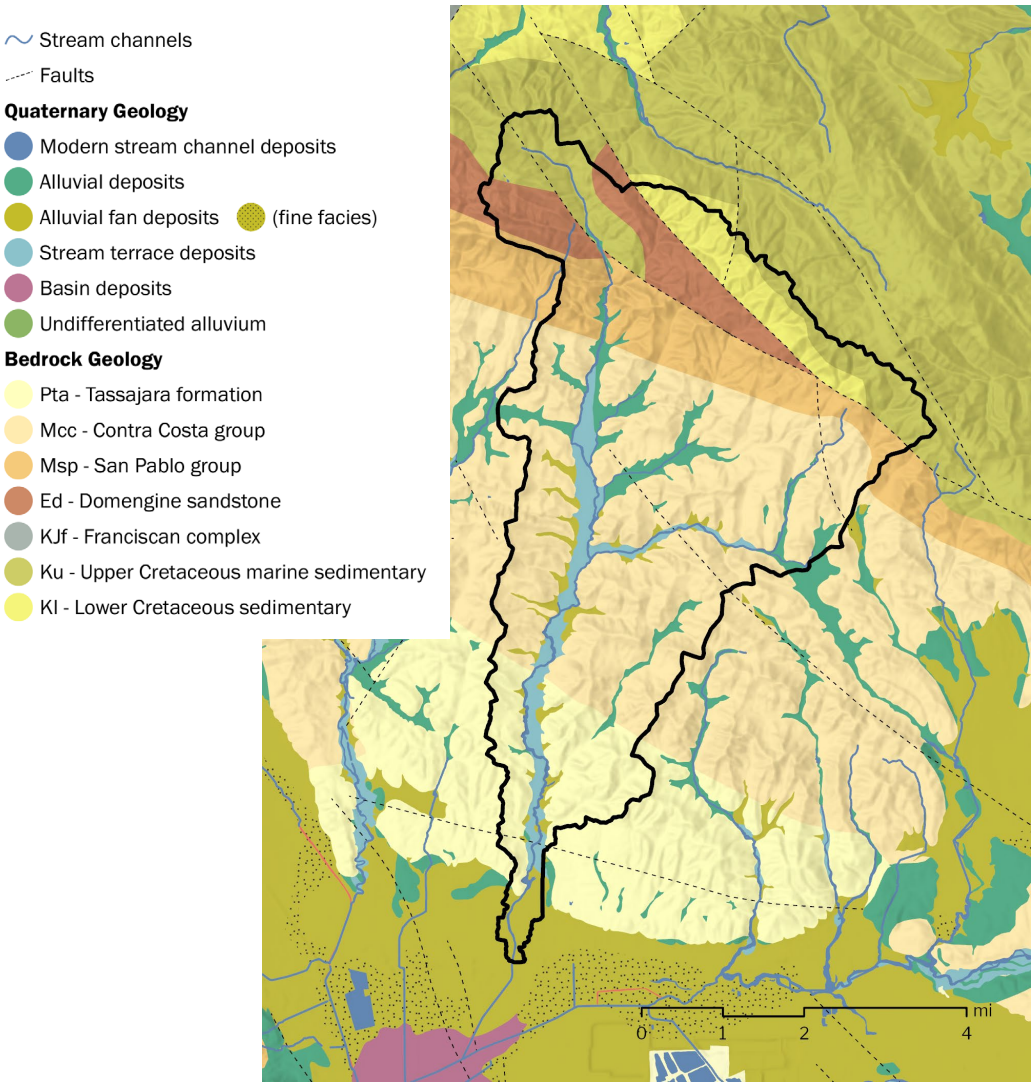

(Knudsen et al., 2000; Ludington et al., 2005)

(b) Hydrologic Soil Groups

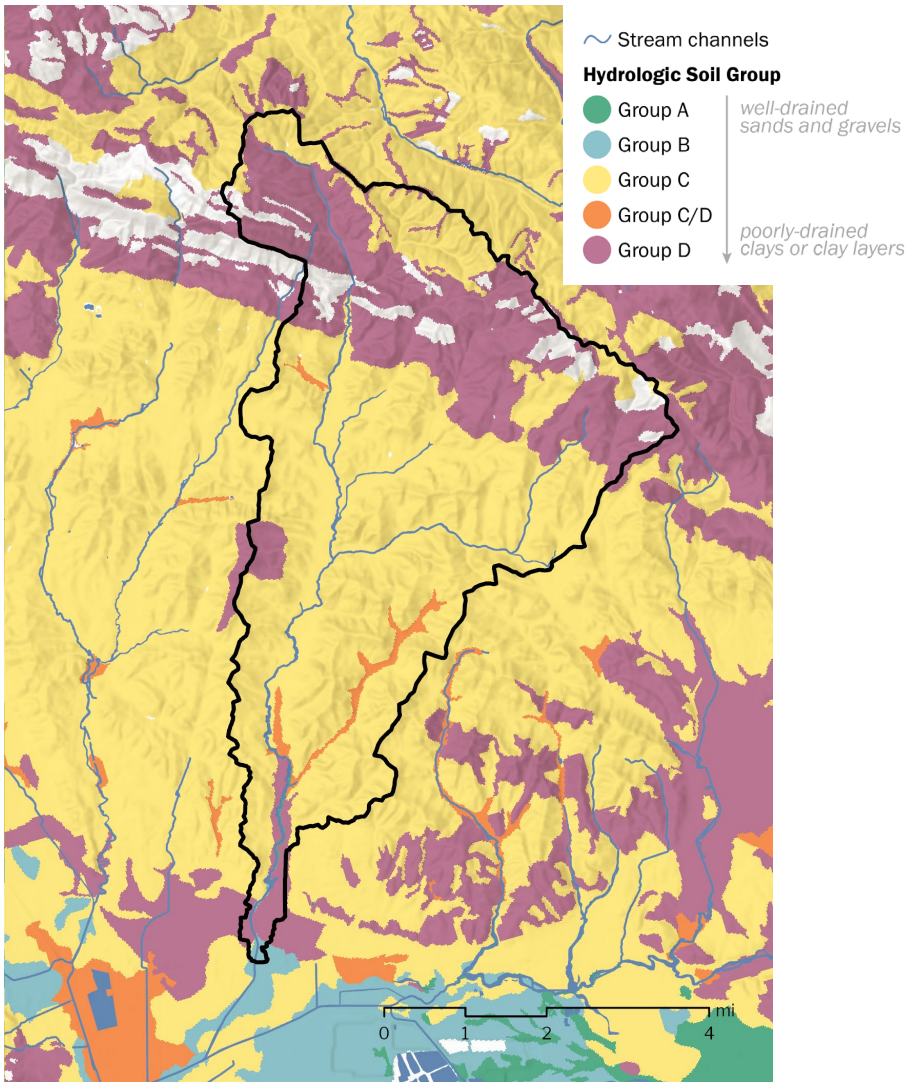

(USGS SSURGO via Esri World Atlas)

Figure 8. Early maps indicating the alignment of Tassajara Creek, 1873 and 1878

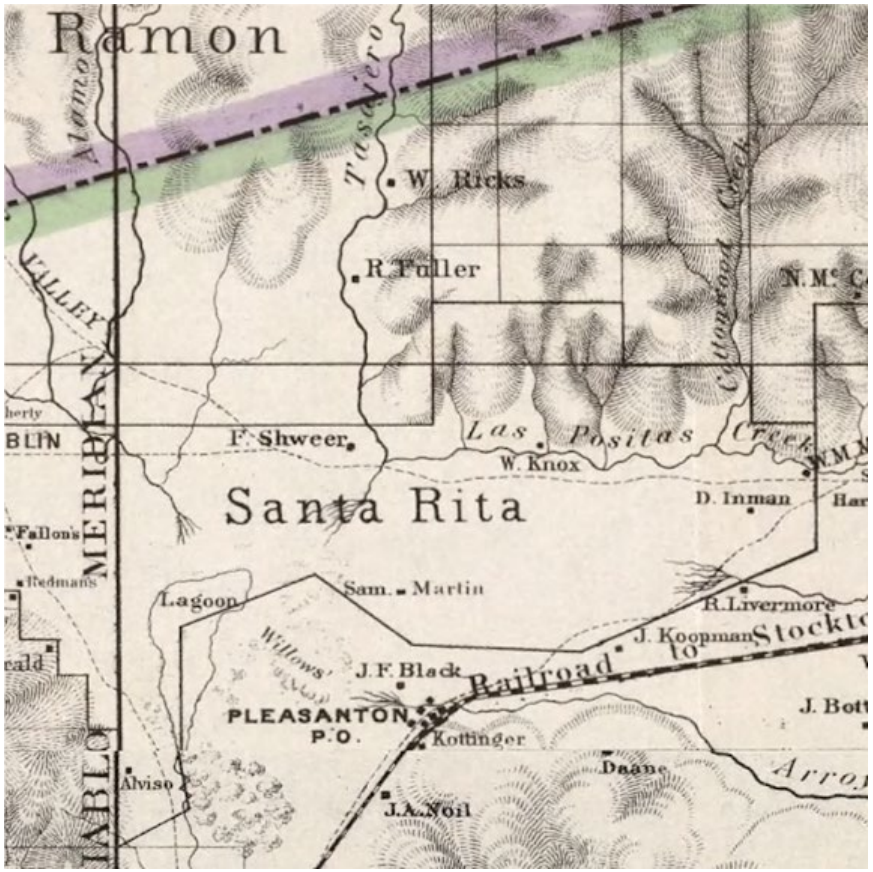

(Hoffmann & Whitney, 1873)

(Thompson & West, 1878)

Figure 9. Land Use and Land Cover, Tassajara Creek basin

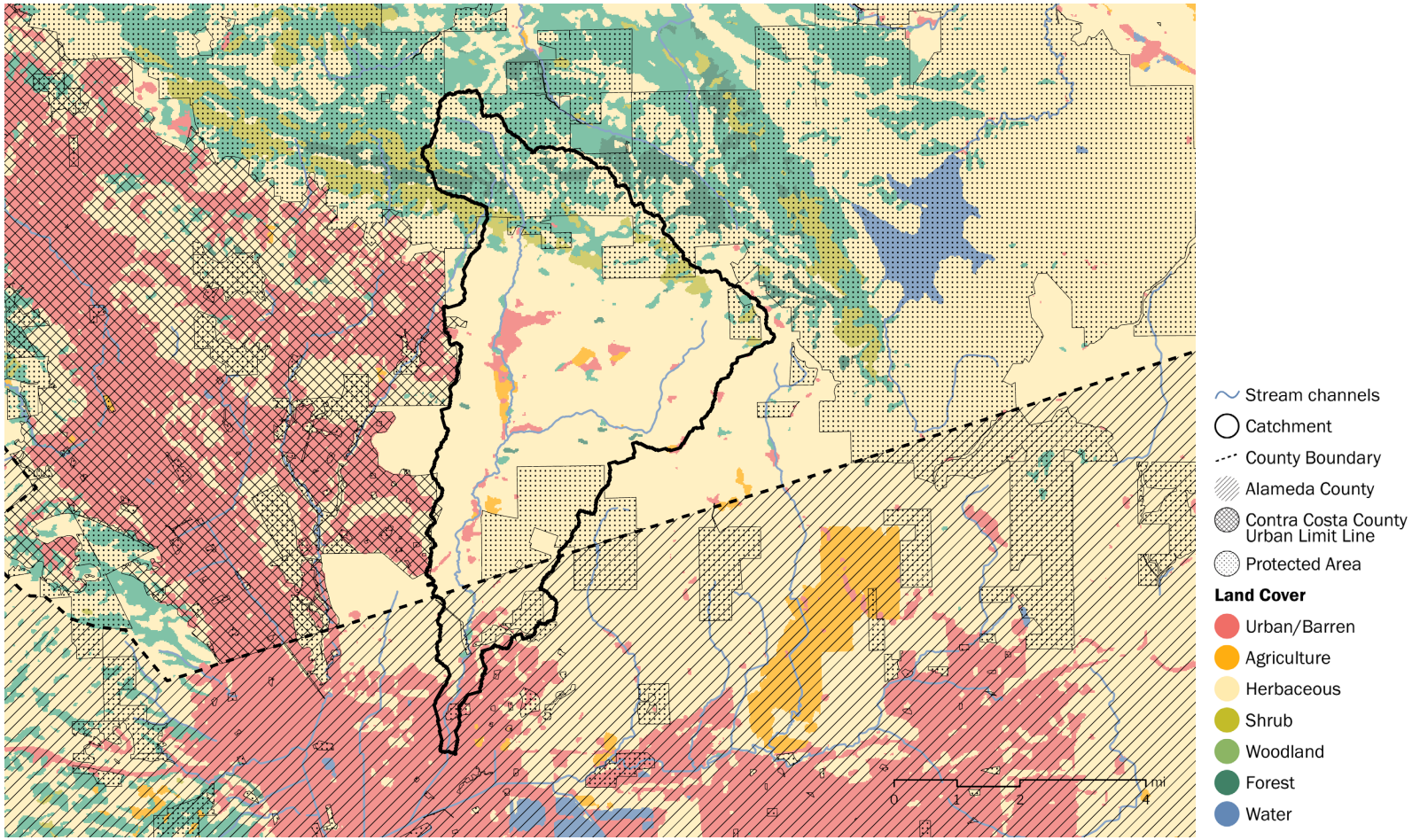

Sources: CALFIRE FRAP (land cover); California Protected areas Database; Contra Costa County and Alameda County

Figure 10. Lower Tassajara Creek effective catchment including stormwater infrastructure

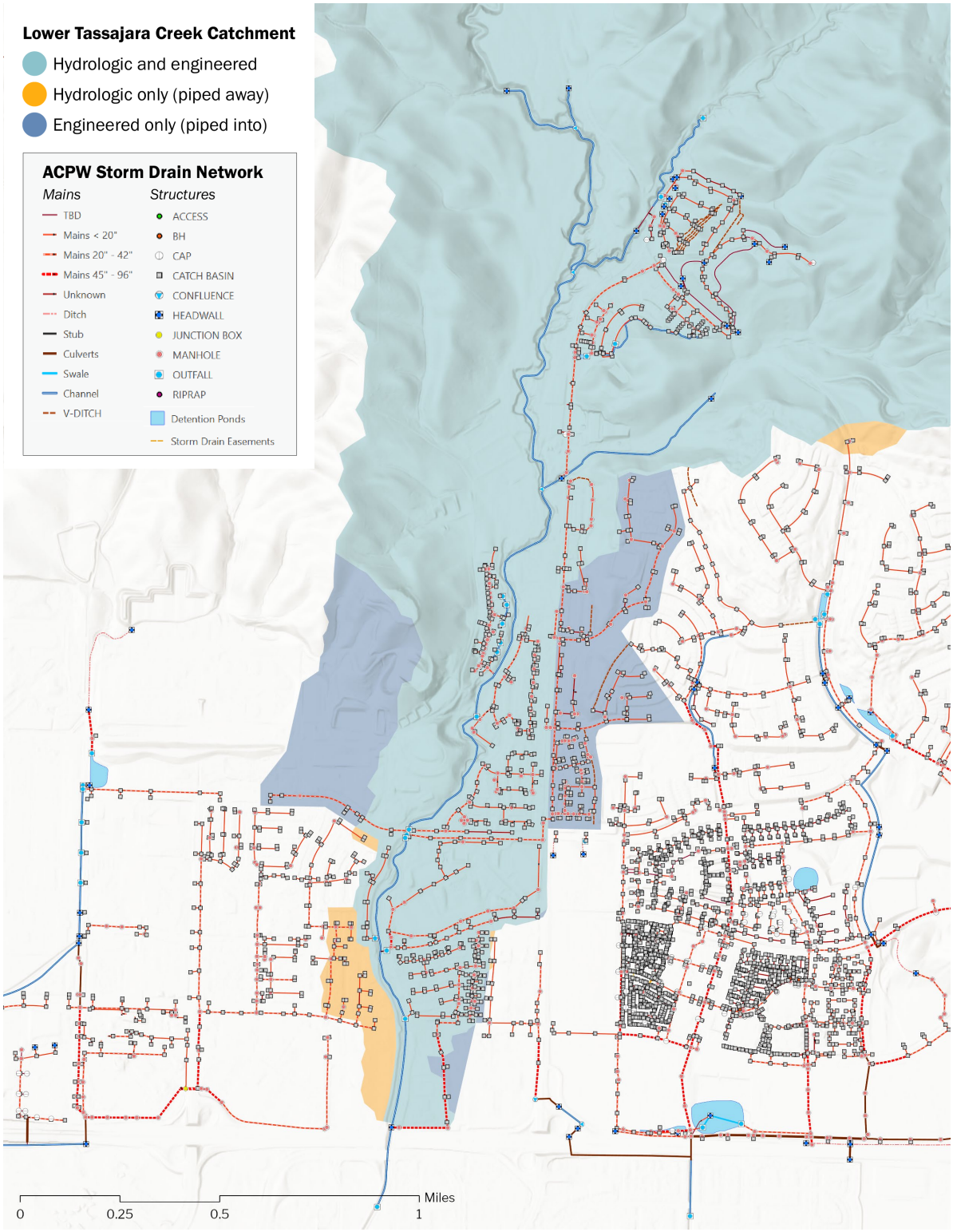

Storm drain map source: City of Dublin Public Works / Tim Eisler / Lynx Technologies

Figure 11. Post-restoration photo time series panorama: 2001, 2021

Figure 12. 2021 LiDAR, raw and detrended

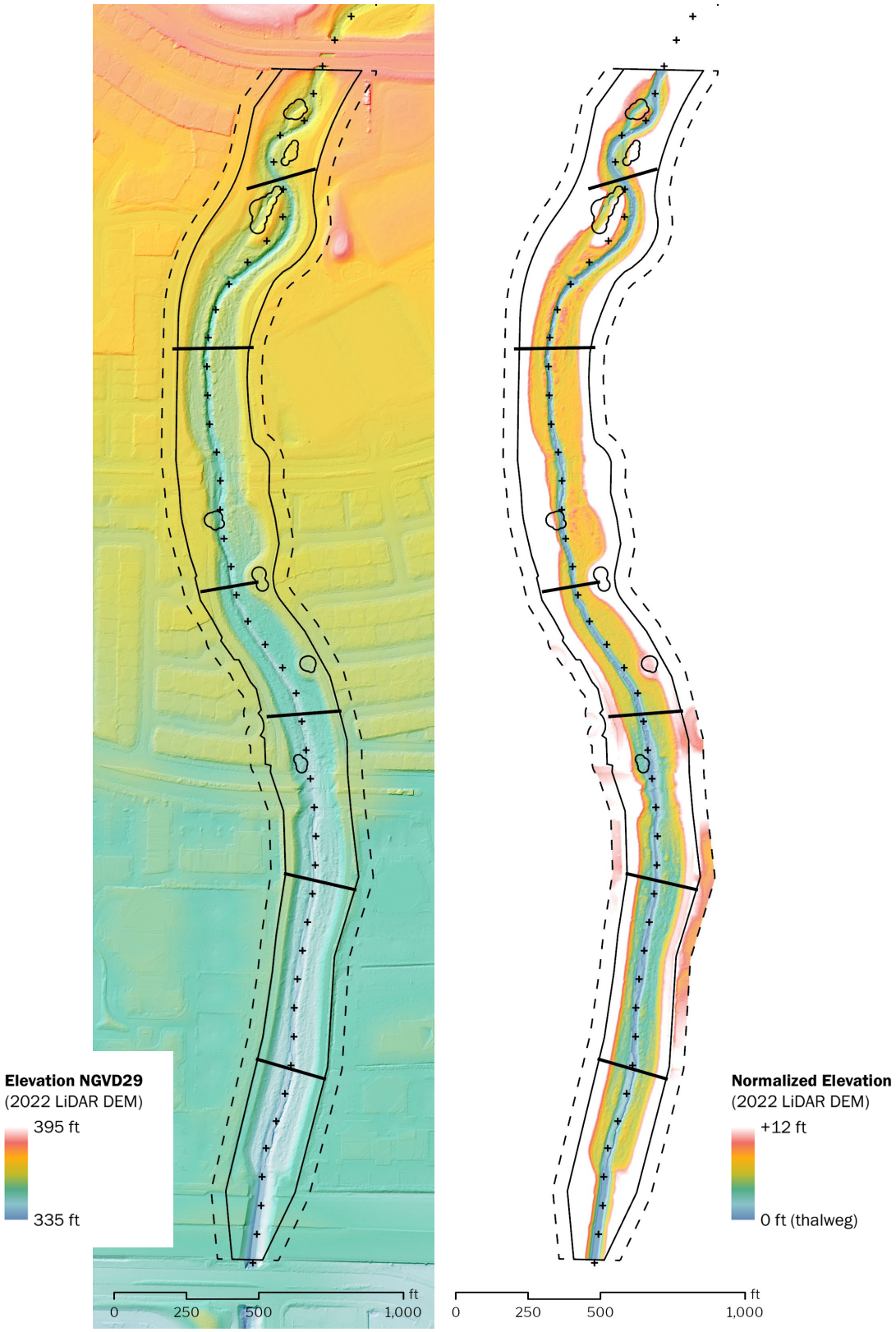

Figure 13. Cross section survey results

(b) XS B: upper reach, south of Gleason Dr (looking downstream)

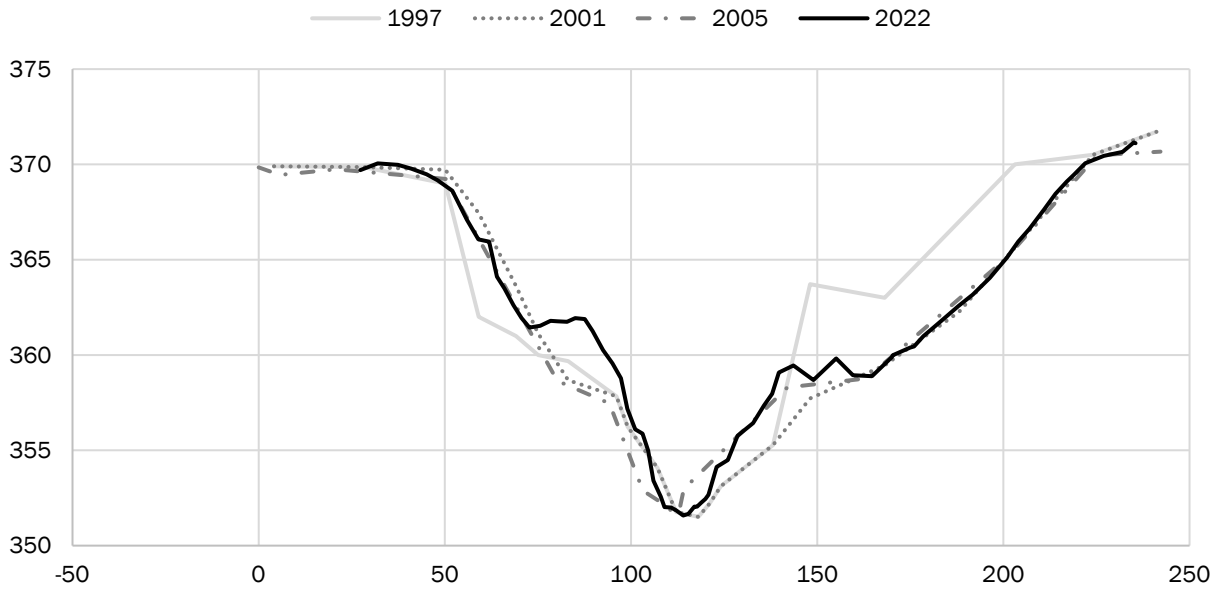

(d) XS D: middle reach, north of Central Pkwy (looking downstream)

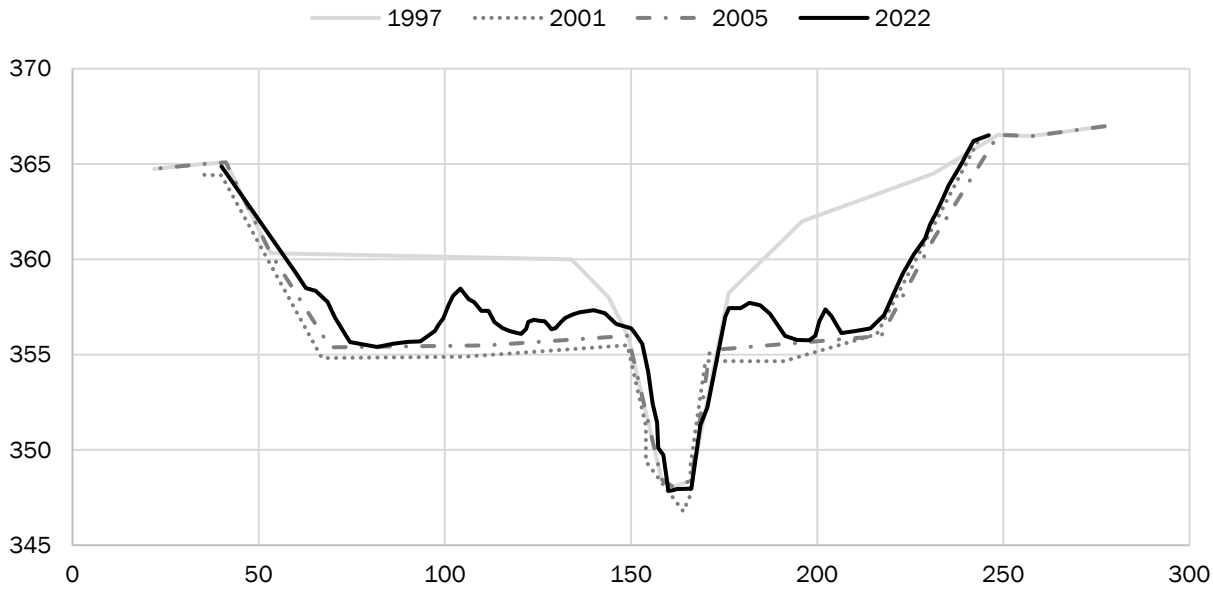

(e) XS E: middle reach, south of Central Pkwy (looking downstream)

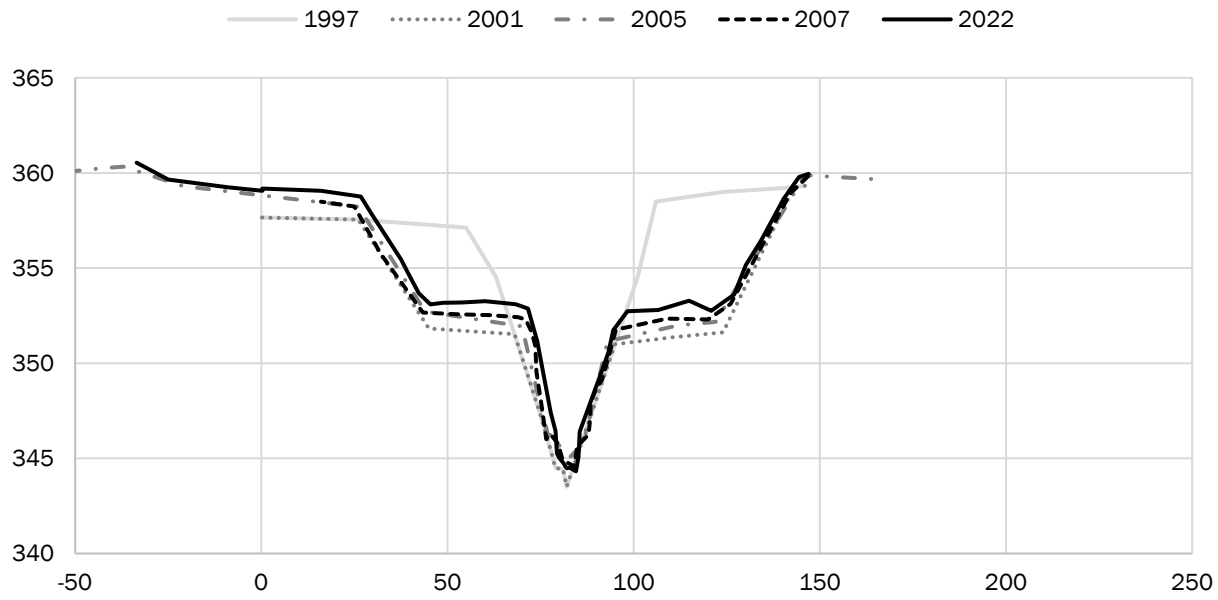

(f) XS F: middle reach, north of Dublin Blvd (looking downstream)

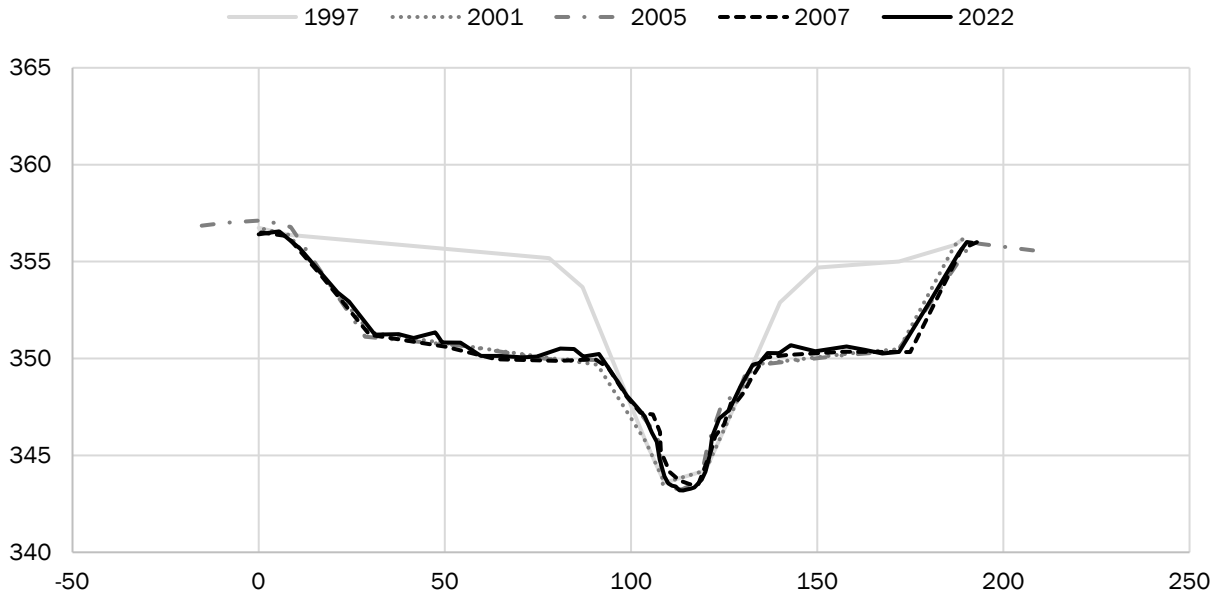

(g) XS G: lower reach, south of Dublin Blvd (looking downstream)

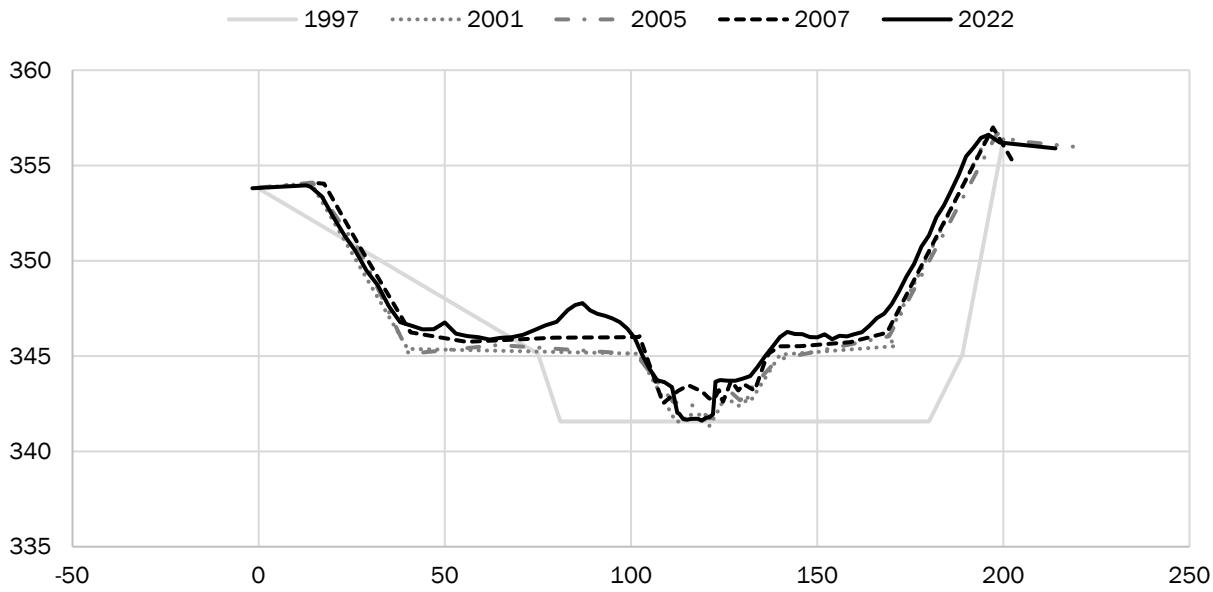

(h) XS H: lower reach, north of I-580 (looking downstream)

Figure 14. Longitudinal profile overview with prior results

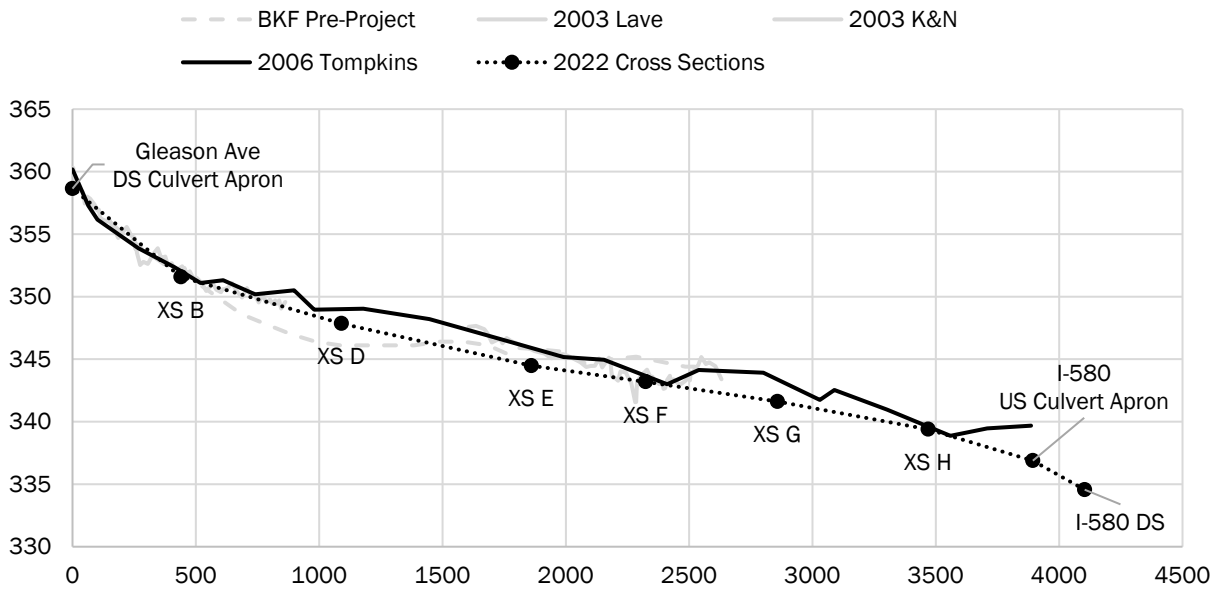

Figure 15. Longitudinal profile south from Gleason Dr (2022)

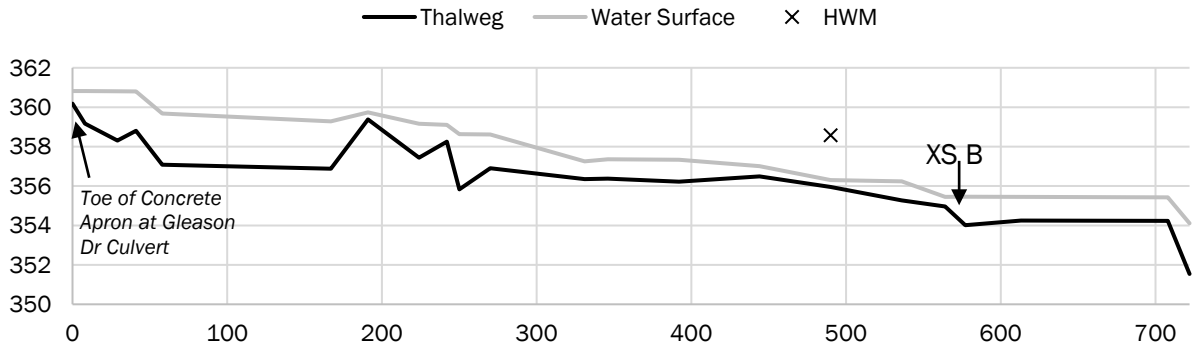

Figure 16. Longitudinal profile from Dublin Blvd to I-580 (2022)

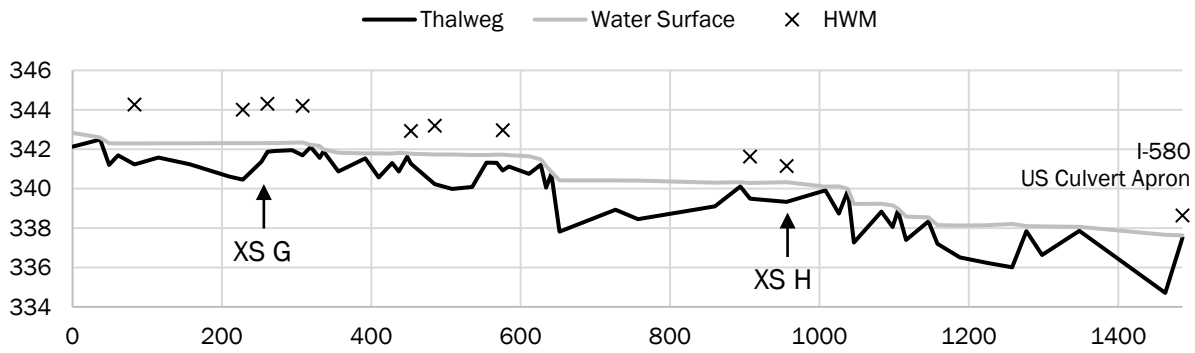

Figure 17. Field sketch of low flow channel conditions at Cross Section B

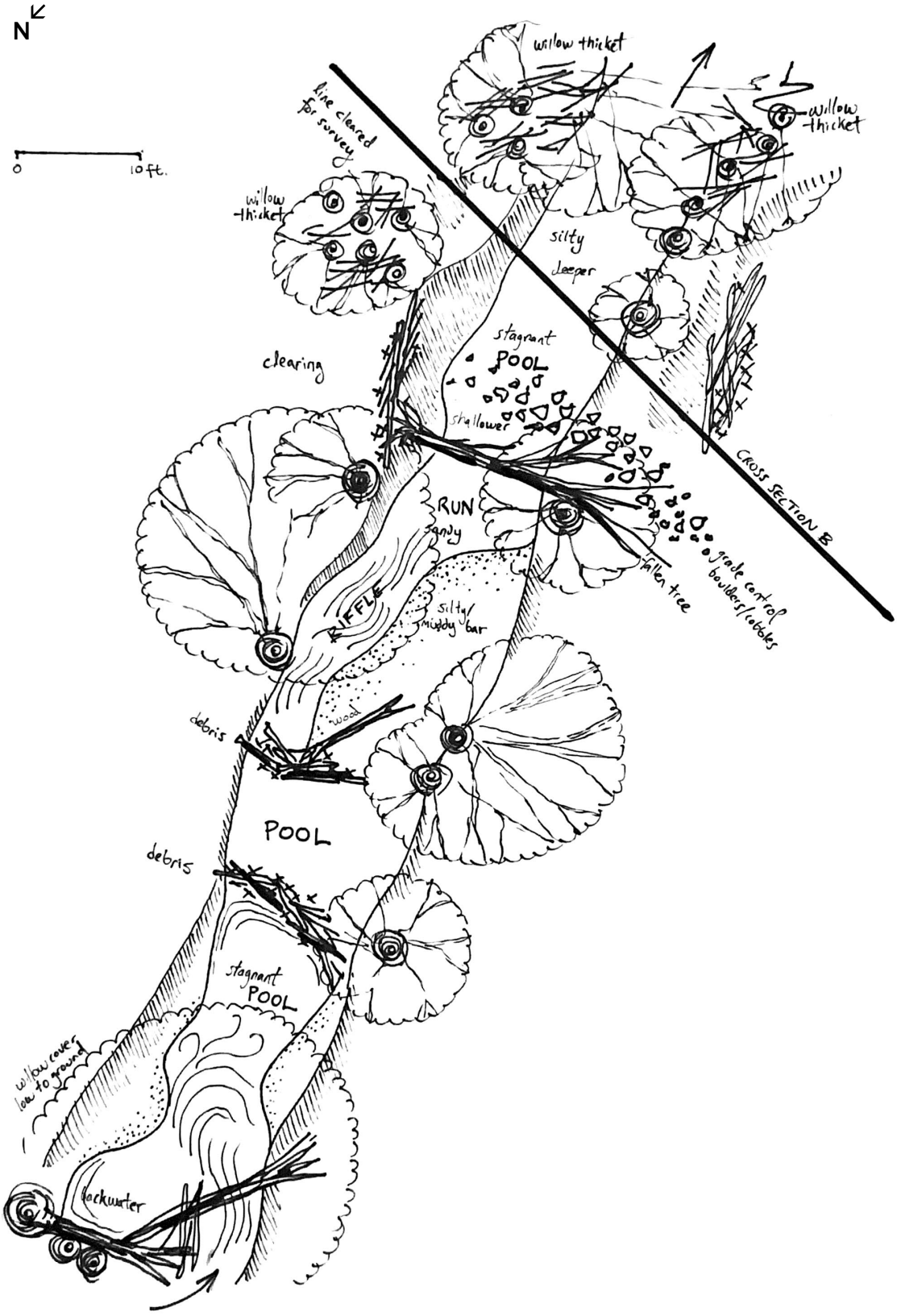

Figure 18. Photograph of low flow channel conditions at Cross Section B

looking downstream toward XS B from the channel thalweg

Figure 19. Photograph of low flow channel conditions at Cross Section E

looking upstream toward XS E from the right bank

Figure 20. Field sketch and photograph of low flow channel conditions at Cross Section H

XS H planimetric field sketch (planimetric, digitally sketched on tablet, approximate scale)

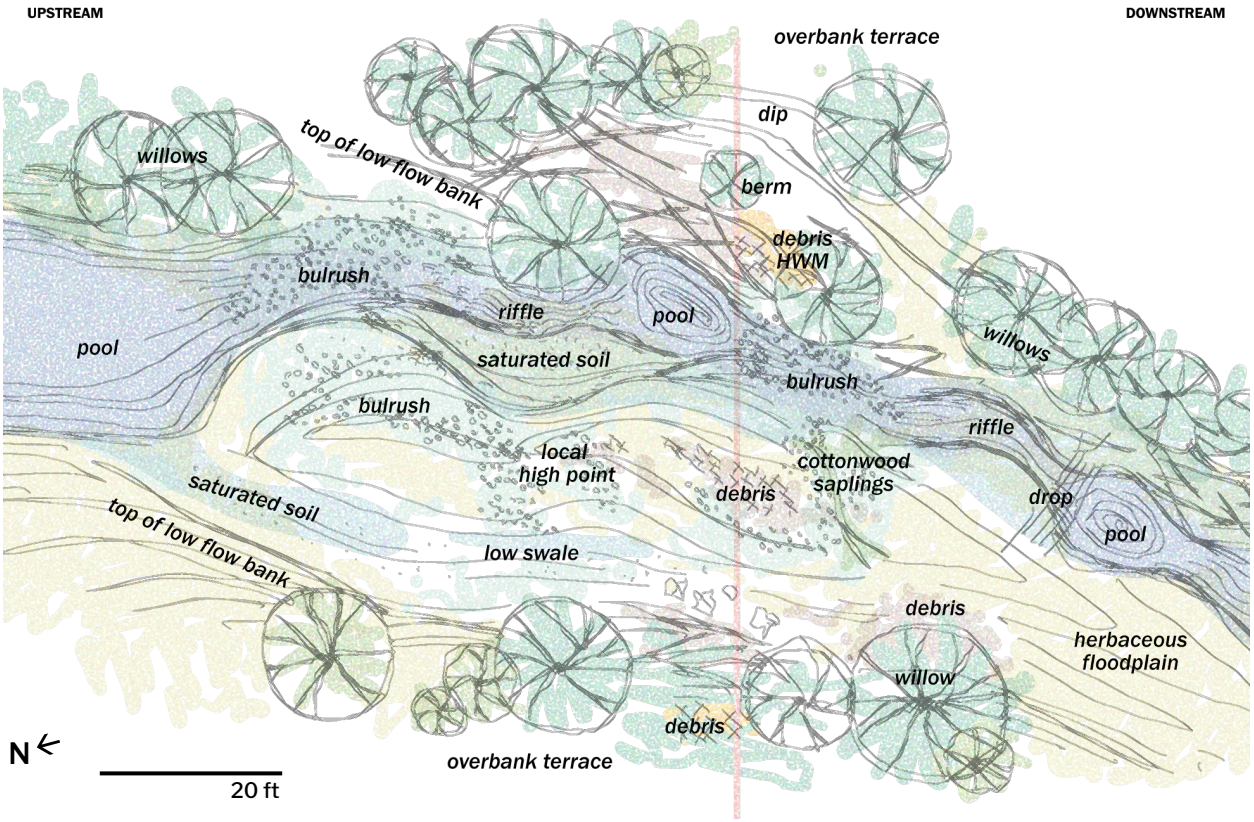

Panoramic photograph of XS H low flow channel (looking downstream)

Figure 21. HEC-RAS longitudinal results

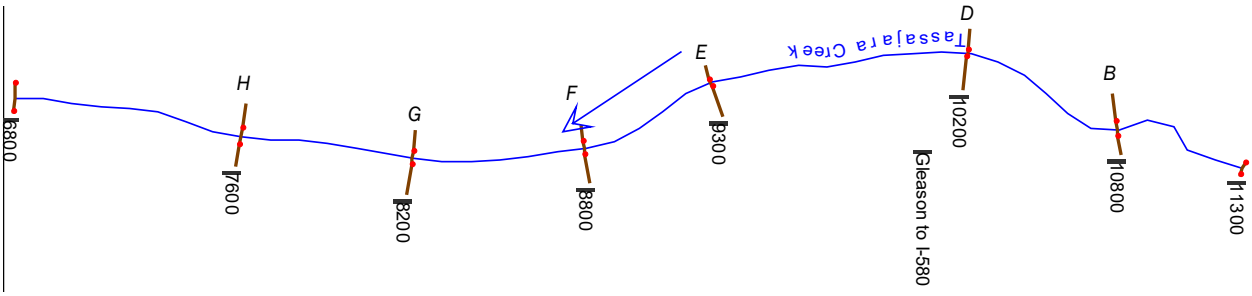

Modeled water surface elevation

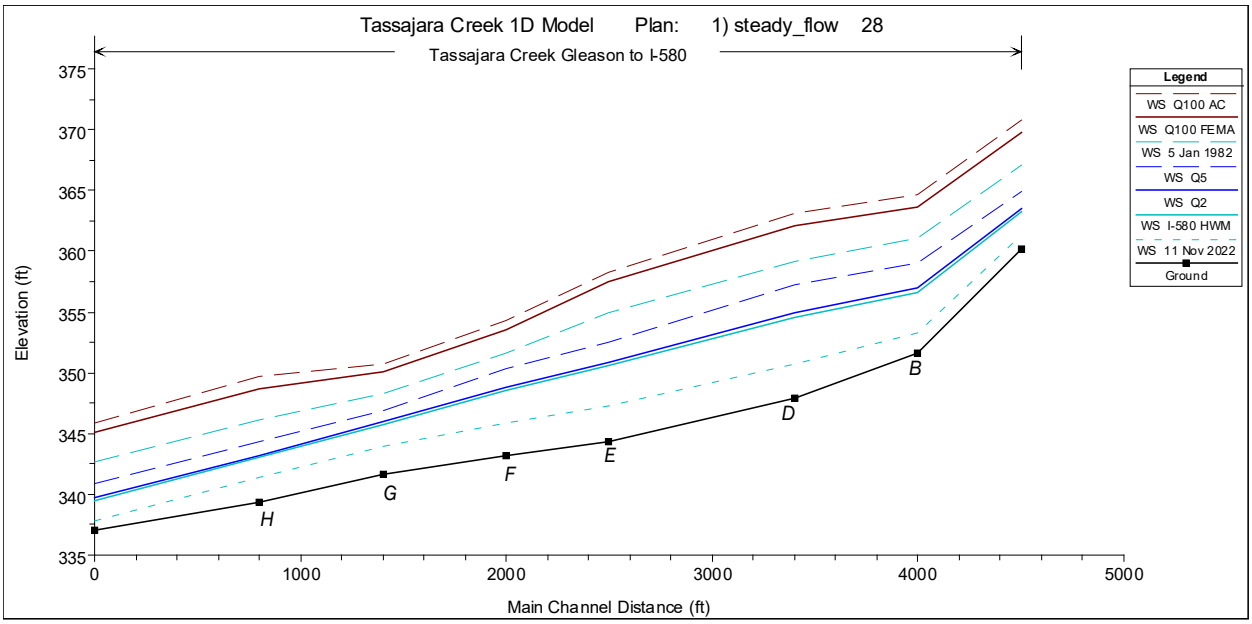

Flow velocities in channel (upper) and on floodplain (lower)

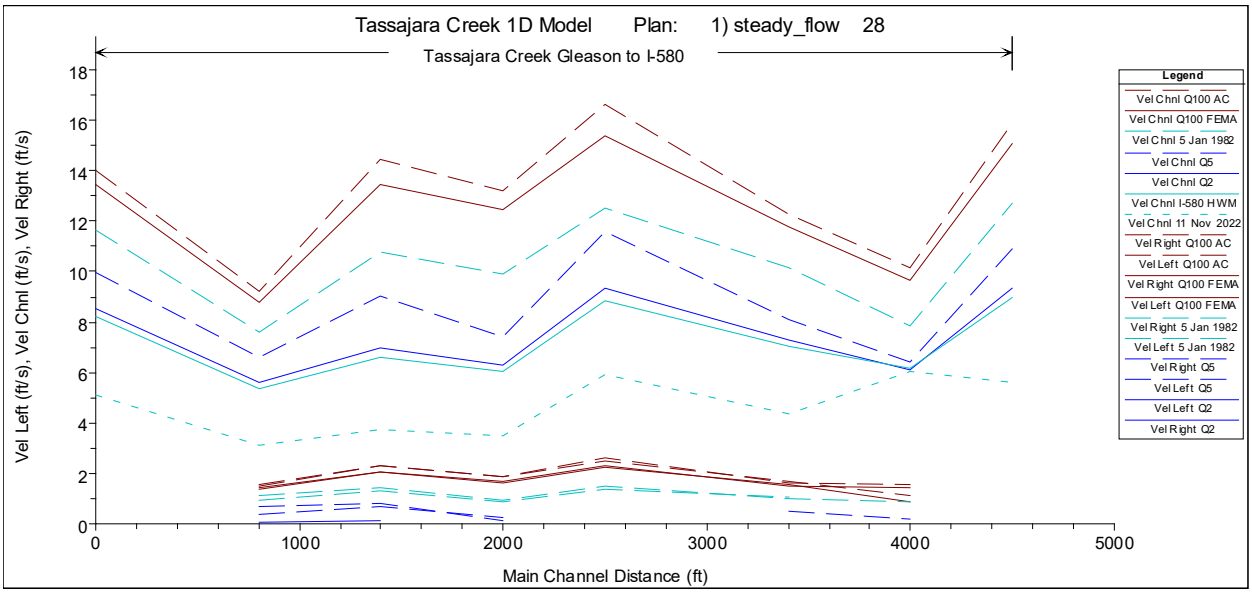

Figure 22. HEC-RAS 1D model results by cross section

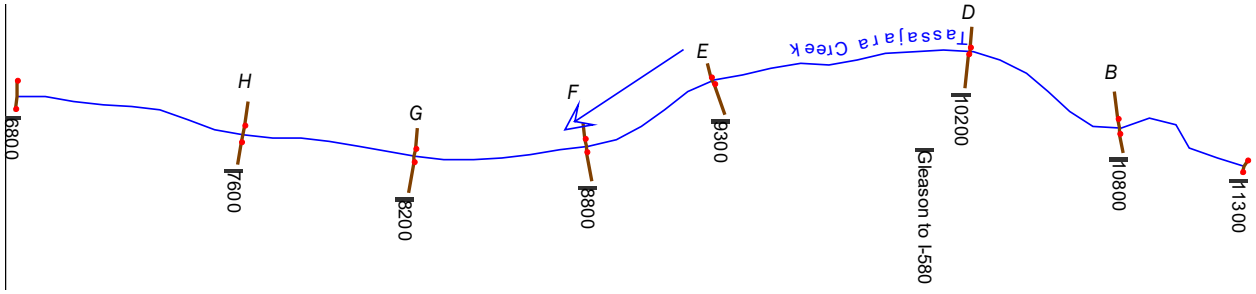

XS B: upper reach, south of Gleason Dr

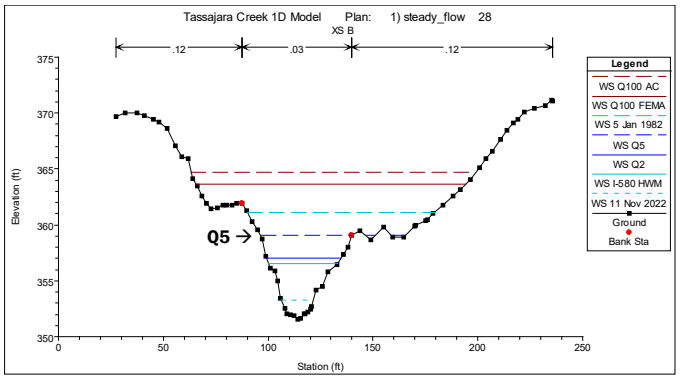

XS D: middle reach, north of Central Pkwy

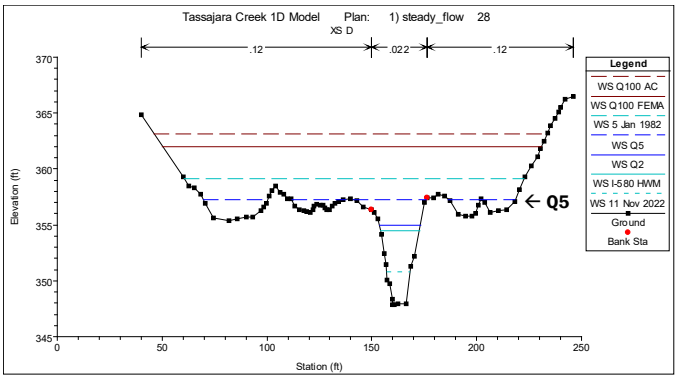

XS E: middle reach, south of Central Pkwy

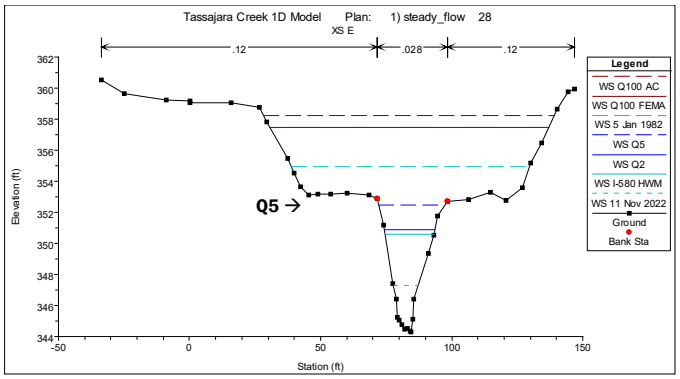

XS F: middle reach, north of Dublin Blvd

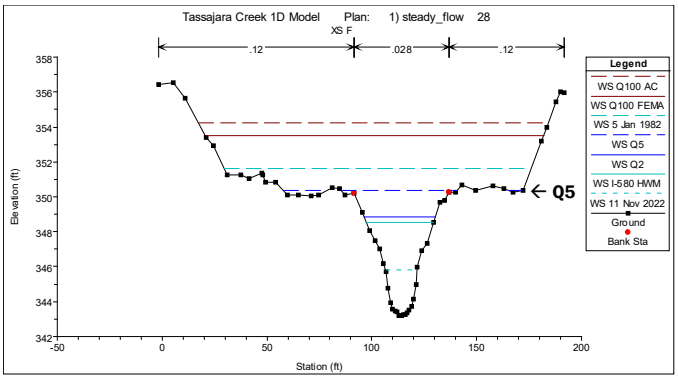

XS G: lower reach, south of Dublin Blvd

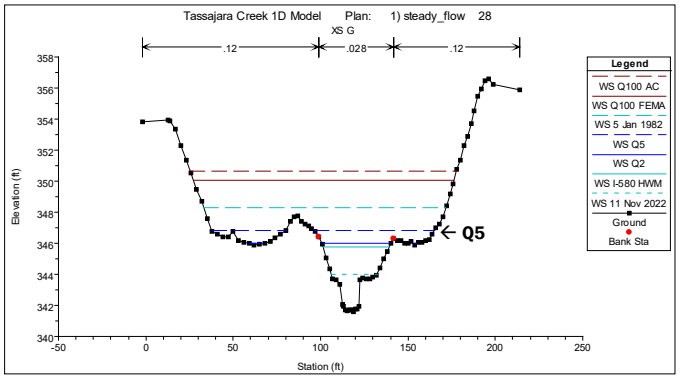

XS H: lower reach, north of I-580

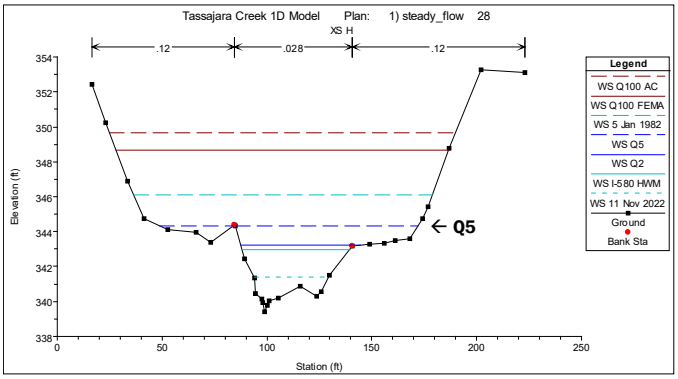

Figure 23. 100-year freeboard estimates by cross section

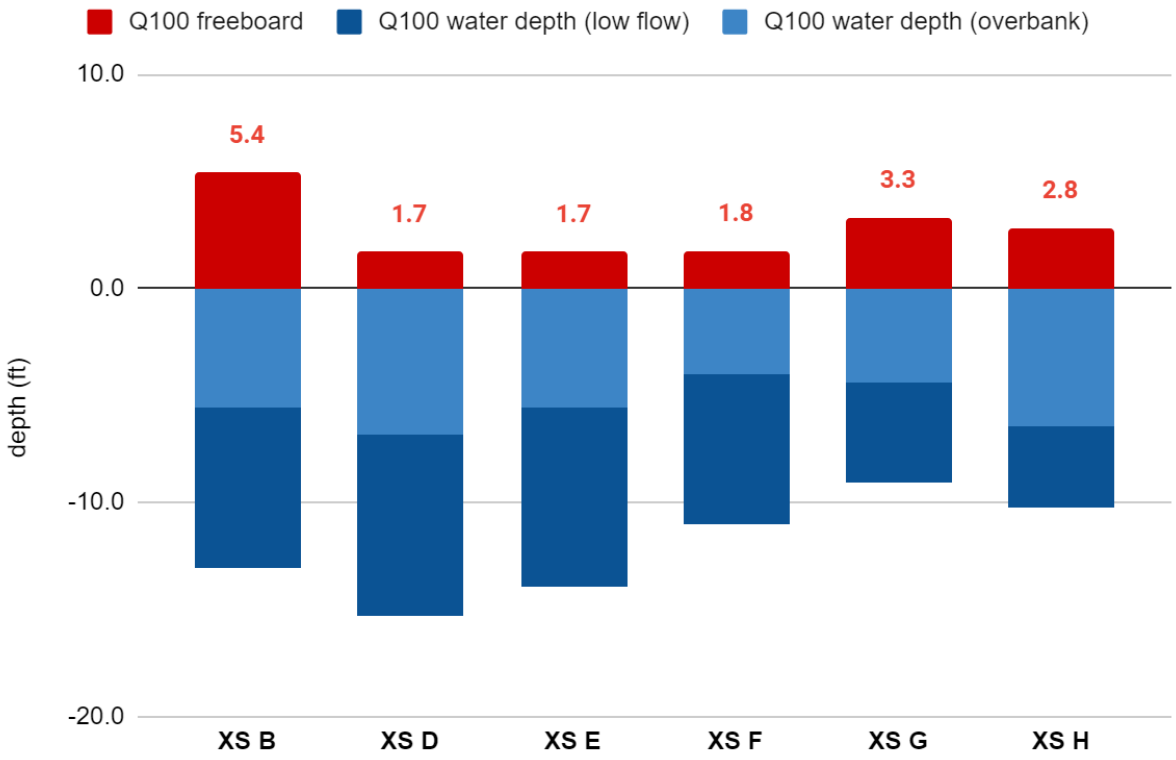

Figure 24. Depth-discharge rating curves and bankfull estimates by cross section

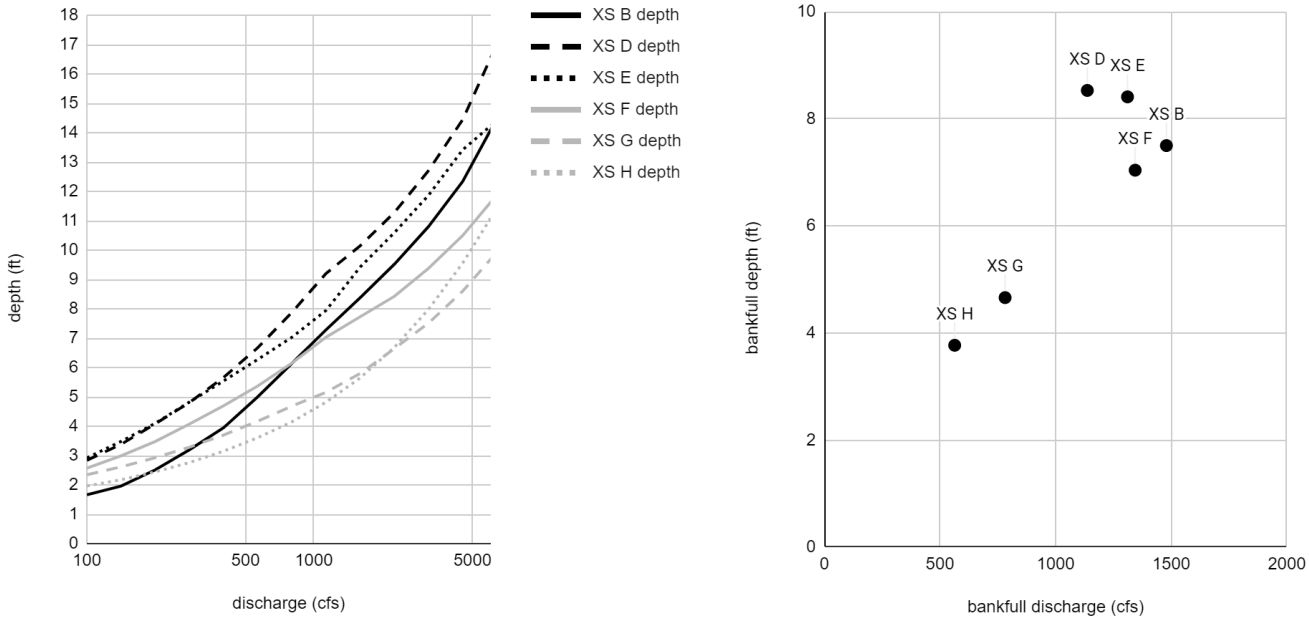

Figure 25. Approximate interpolated flow frequency relations for Lower Tassajara Creek

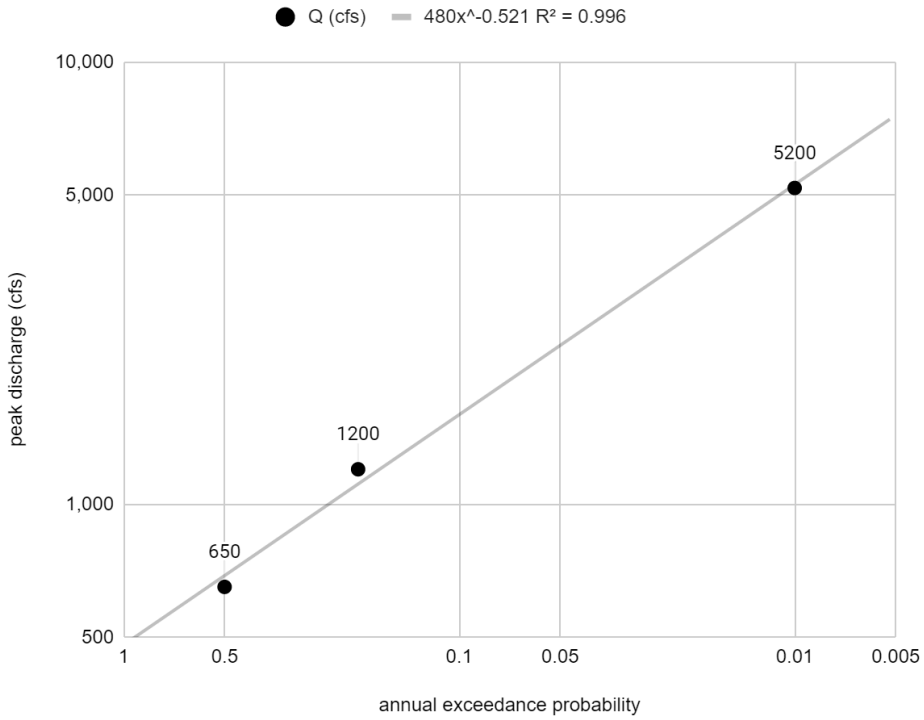

Figure 26. LiDAR differencing result

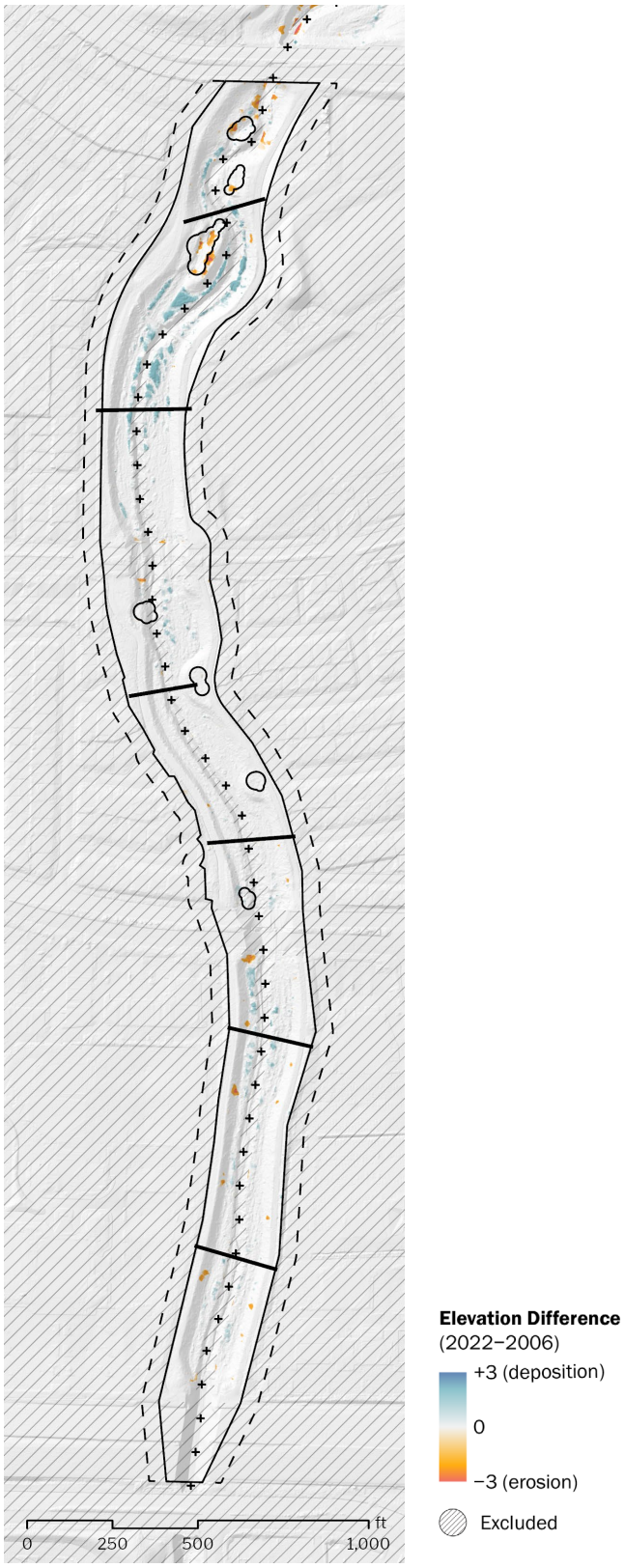

Figure 27. Potential depositional landform at XS B left bank

Section cut:

Sediment just below surface:

Sediment 2 ft below surface:

Figure 28. Other potential depositional landforms

Downstream of promontory in upper reach:

On XS D left bank floodplain:

Figure 29. Peak flow recurrence intervals for San Ramon Creek at Bollinger Canyon

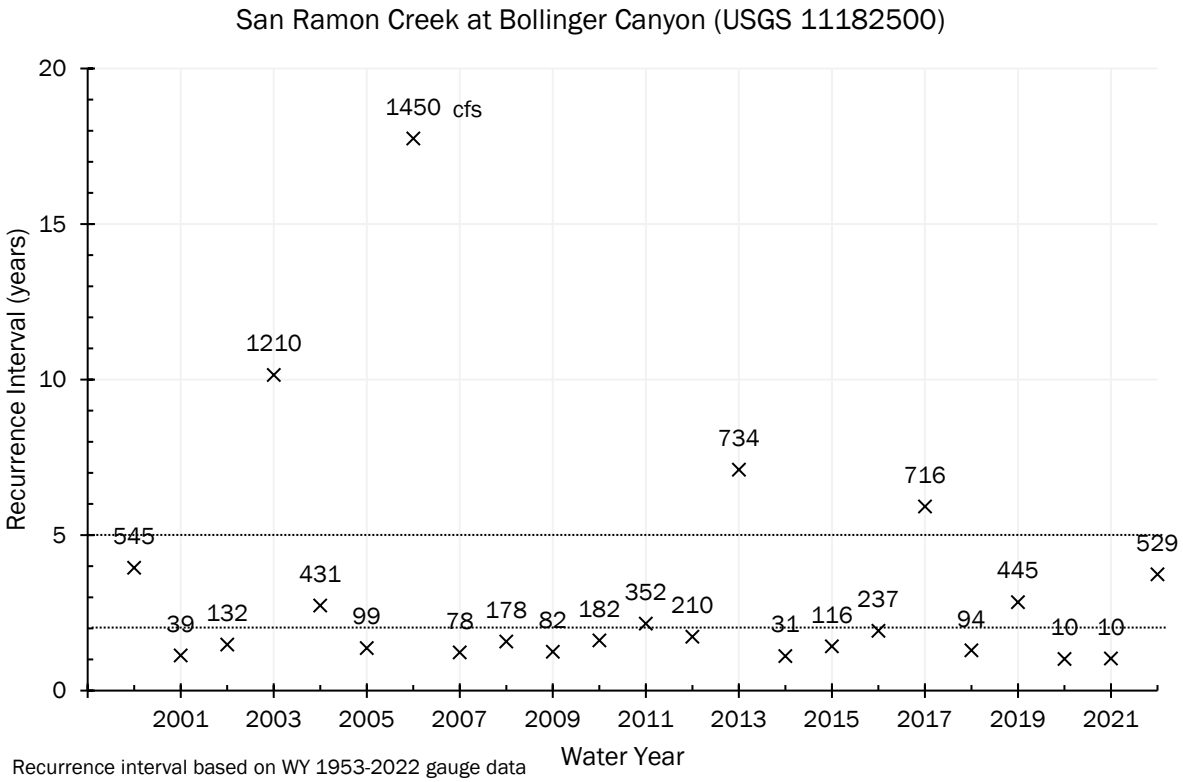

Appendix A: Geospatial Models

LiDAR Comparison

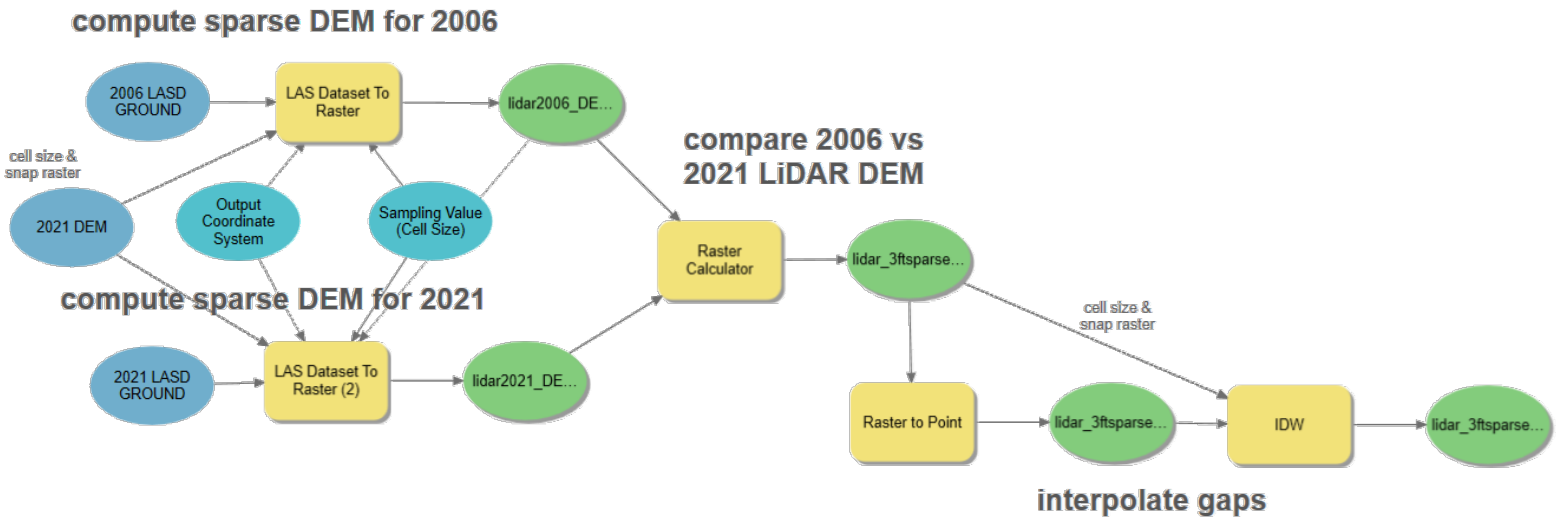

Appendix B: Survey Data Tables

- Cross sections B, D, E, F, G, H
- Interstate 580 high water mark survey
- Longitudinal profile: upper reach south of Gleason Dr
- Longitudinal profile: lower reach Dublin Blvd to Interstate 580

Cross Section B (27 July 2022)

BM / TP	STA from RB	STA from LB	BS+	HI	FS-	ELEV	WD	WSE
BM COD Mon. @XSBC						370.04		
			4.13	374.17				
BM XSC RB					4.03	370.14		
BM XSB RB	1.5	235.5			3.06	371.11		
	2.0	235.0			3.02	371.15		
	5.0	232.0			3.51	370.66		
	10.0	227.0			3.72	370.45		
	15.0	222.0			4.11	370.06		
	18.0	219.0			4.70	369.47		
	20.0	217.0			5.07	369.10		
	23.0	214.0			5.71	368.46		
	26.1	210.9			6.54	367.63		
	30.0	207.0			7.55	366.62		
	33.0	204.0			8.22	365.95		
	36.0	201.0			9.05	365.12		
	40.6	196.4			10.12	364.05		
	45.2	191.8			11.00	363.17		
	49.0	188.0			11.59	362.58		
	53.8	183.2			12.40	361.77		
	58.5	178.5			13.18	360.99		
TP	61.0	176.0			13.72	360.45		
	62.0	175.0			13.78	360.39		
	66.7	170.3			14.18	359.99		
			2.92	363.37				
	67.0	170.0			3.49	359.88		
	72.3	164.7			4.48	358.89		
	77.4	159.6			4.43	358.94		
	81.9	155.1			3.55	359.82		
	88.0	149.0			4.68	358.69		
	93.4	143.6			3.92	359.45		
	97.3	139.7			4.29	359.08		
	99.1	137.9			5.40	357.97		
	101.3	135.7			6.02	357.35		
	104.2	132.8			6.94	356.43		
	108.4	128.6			7.60	355.77		
	111.0	126.0			8.88	354.49		
	114.0	123.0			9.24	354.13		
	116.2	120.8			10.70	352.67		
	117.0	120.0			10.92	352.45	0.00	352.45
	118.2	118.8			11.13	352.24	0.12	352.36
	119.3	117.7			11.33	352.04	0.30	352.34
	120.0	117.0			11.32	352.05	0.31	352.36
	121.6	115.4			11.71	351.66	0.70	352.36
	123.0	114.0			11.79	351.58	0.80	352.38
	124.8	112.2			11.53	351.84	0.49	352.33
	126.2	110.8			11.37	352.00	0.38	352.38
	128.0	109.0			11.35	352.02	0.31	352.33
	129.0	108.0			10.80	352.57	0.00	352.57
	131.0	106.0			9.96	353.41		
	132.4	104.6			8.38	354.99		
	133.9	103.1			7.49	355.88		
	135.9	101.1			7.27	356.10		
	138.0	99.0			6.19	357.18		
	139.7	97.3			4.59	358.78		
	142.0	95.0			3.81	359.56		
	144.5	92.5			3.11	360.26		

BM / TP	STA from RB	STA from LB	BS+	HI	FS-	ELEV	WD	WSE
	147.3	89.7			2.11	361.26		
	149.4	87.6			1.48	361.89		
	152.0	85.0			1.43	361.94		
	154.2	82.8			1.63	361.74		
	156.7	80.3			1.60	361.77		
	158.6	78.4			1.58	361.79		
TP	161.4	75.6			1.84	361.53		
			9.73	371.26				
	164.3	72.7			9.82	361.44		
	166.4	70.6			9.32	361.94		
	168.6	68.4			8.64	362.62		
	171.0	66.0			7.77	363.49		
	173.0	64.0			7.15	364.11		
	175.1	61.9			5.31	365.95		
	178.0	59.0			5.19	366.07		
	181.1	55.9			4.16	367.10		
	185.0	52.0			2.64	368.62		
	189.0	48.0			2.09	369.17		
	191.9	45.1			1.78	369.48		
	196.0	41.0			1.48	369.78		
	199.6	37.4			1.28	369.98		
	205.0	32.0			1.21	370.05		
	209.7	27.3			1.56	369.70		
2022-08-31 ADD MEASUREMENTS OF HWMs:								
BM XSB RB	1.5	235.5				371.11		
			3.86	374.97				
TP	49.0	188.0			12.42	362.55		
			0.22	362.77				
HWM1					7.05	355.72		
HWM2					7.23	355.54		
HWM3					4.79	357.98		

Cross Section D (20 July 2022)

BM / TP	STA from RB	STA from LB	BS+	HI	FS-	ELEV	WD	WSE
BM COD Mon. @XSD						365.88		
			4.05	369.93				
BM XSD RB1					3.19	366.74		
BM XSD RB2	27.9	246.1			3.42	366.51		
	32.0	242.0			3.72	366.21		
	33.9	240.1			4.40	365.53		
	35.1	238.9			4.86	365.07		
	36.7	237.3			5.39	364.54		
	38.7	235.3			6.05	363.88		
	40.1	233.9			6.68	363.25		
	42.0	232.0			7.48	362.45		
	43.7	230.3			8.10	361.83		
	45.0	229.0			8.84	361.09		
	48.0	226.0			9.65	360.28		
	51.0	223.0			10.67	359.26		
	53.5	220.5			11.74	358.19		
	56.0	218.0			12.85	357.08		
	59.7	214.3			13.56	356.37		
	63.7	210.3			13.69	356.24		
	67.5	206.5			13.80	356.13		
	70.2	203.8			12.90	357.03		
	71.8	202.2			12.56	357.37		
	73.4	200.6			13.18	356.75		
	74.5	199.5			13.93	356.00		
	76.1	197.9			14.18	355.75		
	79.4	194.6			14.16	355.77		
	82.6	191.4			13.95	355.98		
	86.7	187.3			12.78	357.15		
	89.3	184.7			12.34	357.59		
	92.2	181.8			12.21	357.72		
	94.5	179.5			12.49	357.44		
	97.7	176.3			12.49	357.44		
	98.7	175.3			12.94	356.99		
HWM	103.5	170.5			16.57	353.36		
	103.5	170.5			17.70	352.23		
	105.4	168.6			18.64	351.29		
	107.8	166.2			21.96	347.97		
	111.7	162.3			21.98	347.95	0.58	348.53
	113.1	160.9			22.06	347.87	0.61	348.48
	114.0	160.0			22.08	347.85	0.66	348.51
	114.3	159.7			21.62	348.31	0.18	348.49
	115.3	158.7			20.20	349.73		
	116.7	157.3			19.83	350.10		
	117.0	157.0			18.50	351.43		
	118.2	155.8			17.50	352.43		
	119.4	154.6			15.82	354.11		
	121.0	153.0			14.36	355.57		
	123.0	151.0			13.78	356.15		
TP	124.0	150.0			13.55	356.38		
			8.62	365.00				
	128.0	146.0			8.39	356.61		
	131.0	143.0			7.83	357.17		
	134.0	140.0			7.67	357.33		
	137.8	136.2			7.78	357.22		
	139.7	134.3			7.90	357.10		
	141.7	132.3			8.08	356.92		

BM / TP	STA from RB	STA from LB	BS+	HI	FS-	ELEV	WD	WSE
	142.8	131.2			8.29	356.71		
	144.3	129.7			8.61	356.39		
	145.4	128.6			8.67	356.33		
	146.2	127.8			8.46	356.54		
	147.2	126.8			8.25	356.75		
	148.5	125.5			8.23	356.77		
	150.1	123.9			8.17	356.83		
	151.6	122.4			8.28	356.72		
	152.2	121.8			8.66	356.34		
	153.5	120.5			8.91	356.09		
	155.2	118.8			8.84	356.16		
	156.6	117.4			8.76	356.24		
	158.5	115.5			8.61	356.39		
	160.7	113.3			8.29	356.71		
	162.3	111.7			7.70	357.30		
	164.2	109.8			7.70	357.30		
	166.1	107.9			7.25	357.75		
	167.6	106.4			7.09	357.91		
	169.8	104.2			6.54	358.46		
	171.8	102.2			6.91	358.09		
	173.0	101.0			7.39	357.61		
	174.4	99.6			8.09	356.91		
	175.7	98.3			8.43	356.57		
	176.7	97.3			8.76	356.24		
	180.6	93.4			9.31	355.69		
	184.0	90.0			9.33	355.67		
	188.0	86.0			9.43	355.57		
	192.2	81.8			9.60	355.40		
	199.5	74.5			9.34	355.66		
	203.5	70.5			8.06	356.94		
	205.5	68.5			7.23	357.77		
	208.7	65.3			6.65	358.35		
	211.3	62.7			6.51	358.49		
	214.1	59.9			5.69	359.31		
	234.0	40.0			0.12	364.88		

Cross Section E (10 July 2022)

BM / TP	STA from RB	STA from LB	BS+	HI	FS-	ELEV	WD	WSE
BM XSF RB						355.97		
			5.64	361.61				
TP					2.36	359.25		
			4.28	363.53				
BM XSE RB	46.0	133.0			3.58	359.95		
	48.6	130.4			3.74	359.79		
	52.7	126.3			4.89	358.64		
	58.7	120.3			7.05	356.48		
	62.9	116.1			8.38	355.15		
	66.0	113.0			9.92	353.61		
	72.2	106.8			10.77	352.76		
	78.1	100.9			10.24	353.29		
	86.4	92.6			10.73	352.80		
TP	94.7	84.3			10.80	352.73		
			3.19	355.92				
	98.5	80.5			4.18	351.74		
	99.8	79.2			5.37	350.55		
HWM	100.2	78.8			5.20	350.72		
HWM	101.2	77.8			4.16	351.76		
	102.0	77.0			6.57	349.35		
	107.5	71.5			9.52	346.40		
	107.8	71.2			10.82	345.10	0.70	345.80
	108.5	70.5			11.60	344.32	1.48	345.80
	109.0	70.0			11.54	344.38	1.41	345.79
	110.0	69.0			11.41	344.51	1.26	345.77
	111.0	68.0			11.44	344.48	1.29	345.77
	112.0	67.0			11.13	344.79	1.20	345.99
	113.0	66.0			10.89	345.03	0.76	345.79
	113.6	65.4			10.66	345.26	0.51	345.77
	114.0	65.0			9.48	346.44		
	115.3	63.7			8.51	347.41		
	118.9	60.1			4.77	351.15		
	121.4	57.6			3.05	352.87		
	124.7	54.3			2.82	353.10		
	132.9	46.1			2.66	353.26		
	139.1	39.9			2.73	353.19		
	144.2	34.8			2.74	353.18		
TP	147.6	31.4			2.83	353.09		
			7.91	361.00				
	150.7	28.3			7.33	353.67		
	153.0	26.0			6.48	354.52		
	155.5	23.5			5.54	355.46		
	163.4	15.6			3.15	357.85		
	166.3	12.7			2.24	358.76		
	177.0	2.0			1.94	359.06		
BM XSF LB	192.7	-13.7			1.82	359.18		
	192.7	-13.7			1.94	359.06		
	202.0	-23.0			1.75	359.25		
	218.0	-39.0			1.35	359.65		
	226.5	-47.5			0.46	360.54		

Cross Section F (10 July 2022)

BM / TP	STA from RB	STA from LB	BS+	HI	FS-	ELEV	WD	WSE
BM TOWILL						356.46		
			3.14	359.60				
BM XSF RB	29.4	191.6			3.63	355.97		
			0.04	356.01				
	30.8	190.2			0.00	356.01		
	33.0	188.0			0.58	355.43		
	37.5	183.5			2.03	353.98		
	40.0	181.0			2.84	353.17		
	49.0	172.0			5.67	350.34		
	53.5	167.5			5.75	350.26		
	58.2	162.8			5.56	350.45		
	63.1	157.9			5.39	350.62		
	71.5	149.5			5.64	350.37		
	78.1	142.9			5.32	350.69		
	81.2	139.8			5.74	350.27		
	84.3	136.7			5.73	350.28		
	86.5	134.5			6.24	349.77		
	88.3	132.7			6.33	349.68		
	91.7	129.3			7.49	348.52		
	94.6	126.4			8.67	347.34		
	97.3	123.7			9.11	346.90		
	99.2	121.8			10.04	345.97		
	99.9	121.1			11.03	344.98		
	101.0	120.0			11.85	344.16	0.44	344.60
	102.0	119.0			12.26	343.75	0.85	344.60
	103.1	117.9			12.49	343.52	1.10	344.62
	104.0	117.0			12.66	343.35	1.20	344.55
	105.0	116.0			12.73	343.28	1.26	344.54
	106.0	115.0			12.77	343.24	1.34	344.58
	107.0	114.0			12.82	343.19	1.37	344.56
	108.0	113.0			12.81	343.20	1.38	344.58
	109.0	112.0			12.61	343.40	1.19	344.59
	110.0	111.0			12.57	343.44	1.14	344.58
	111.0	110.0			12.46	343.55	1.04	344.59
	112.0	109.0			12.09	343.92	0.66	344.58
	113.3	107.7			11.23	344.78	0.01	344.79
	114.1	106.9			10.31	345.70		
	115.4	105.6			9.83	346.18		
	117.3	103.7			9.00	347.01		
	119.5	101.5			8.50	347.51		
	122.1	98.9			7.93	348.08		
	125.6	95.4			6.91	349.10		
	129.6	91.4			5.78	350.23		
	133.8	87.2			5.91	350.10		
	136.3	84.7			5.52	350.49		
	140.0	81.0			5.50	350.51		
	146.3	74.7			5.91	350.10		
	150.1	70.9			5.95	350.06		
	156.2	64.8			5.88	350.13		
	161.3	59.7			5.88	350.13		
	166.8	54.2			5.19	350.82		
	171.7	49.3			5.18	350.83		
	173.2	47.8			4.75	351.26		
	173.6	47.4			4.66	351.35		
	179.4	41.6			4.95	351.06		
	183.4	37.6			4.75	351.26		

BM / TP	STA from RB	STA from LB	BS+	HI	FS-	ELEV	WD	WSE
	189.8	31.2			4.78	351.23		
	196.7	24.3			3.08	352.93		
	199.8	21.2			2.60	353.41		
TP	209.9	11.1			0.34	355.67		
			4.10	359.77				
	215.5	5.5			3.21	356.56		
BM XSF LB	221.0	0.0			3.36	356.41		

Cross Section G (31 August 2022)

BM / TP	STA from RB	STA from LB	BS+	HI	FS-	ELEV	WD	WSE
BM TOWILL						356.46		
			4.26	360.72				
BM XSG RB	9.0	214.0			4.82	355.90		
			3.48	359.38				
	24.0	199.0			3.17	356.21		
	27.0	196.0			2.77	356.61		
	29.0	194.0			2.93	356.45		
	31.0	192.0			3.44	355.94		
	33.0	190.0			3.90	355.48		
	35.0	188.0			4.87	354.51		
	37.0	186.0			5.70	353.68		
	39.0	184.0			6.48	352.90		
	41.0	182.0			7.10	352.28		
	43.0	180.0			8.05	351.33		
	45.0	178.0			8.64	350.74		
	47.0	176.0			9.54	349.84		
	49.0	174.0			10.20	349.18		
	51.0	172.0			10.98	348.40		
	53.0	170.0			11.66	347.72		
	55.0	168.0			12.15	347.23		
	57.0	166.0			12.39	346.99		
	59.0	164.0			12.79	346.59		
	61.0	162.0			13.13	346.25		
TP	63.0	160.0			13.23	346.15		
			3.85	350.00				
	65.0	158.0			3.97	346.03		
	67.0	156.0			3.93	346.07		
	69.0	154.0			4.12	345.88		
	71.0	152.0			3.86	346.14		
	73.0	150.0			4.02	345.98		
	75.0	148.0			4.00	346.00		
	77.0	146.0			3.85	346.15		
	79.0	144.0			3.84	346.16		
	81.0	142.0			3.73	346.27		
	83.0	140.0			4.00	346.00		
	85.0	138.0			4.51	345.49		
	87.0	136.0			5.01	344.99		
	89.0	134.0			5.56	344.44		
	91.0	132.0			6.05	343.95		
	93.0	130.0			6.18	343.82		
	95.0	128.0			6.29	343.71		
	97.0	126.0			6.29	343.71		
	99.0	124.0			6.26	343.74		
	100.3	122.7			6.34	343.66		
	101.0	122.0			8.05	341.95	0	341.95
	102.0	121.0			8.21	341.79		
	103.0	120.0			8.25	341.75		
	104.0	119.0			8.39	341.61		
	105.0	118.0			8.29	341.71		
	106.0	117.0			8.29	341.71		
	107.0	116.0			8.30	341.70		
	108.0	115.0			8.34	341.66		
	109.0	114.0			8.31	341.69		
	110.0	113.0			8.03	341.97		
	110.6	112.4			7.97	342.03		
	112.0	111.0			6.63	343.37		

BM / TP	STA from RB	STA from LB	BS+	HI	FS-	ELEV	WD	WSE
	114.0	109.0			6.37	343.63		
	116.0	107.0			6.27	343.73		
	118.0	105.0			5.67	344.33		
	120.0	103.0			4.94	345.06		
	122.0	101.0			4.05	345.95		
	124.0	99.0			3.56	346.44		
	126.0	97.0			3.22	346.78		
	128.0	95.0			3.03	346.97		
	130.0	93.0			2.88	347.12		
	132.0	91.0			2.78	347.22		
	134.0	89.0			2.60	347.40		
	136.0	87.0			2.22	347.78		
	138.0	85.0			2.32	347.68		
	140.0	83.0			2.59	347.41		
	143.0	80.0			3.20	346.80		
	146.0	77.0			3.39	346.61		
	149.0	74.0			3.64	346.36		
	152.0	71.0			3.88	346.12		
	155.0	68.0			4.01	345.99		
	158.0	65.0			4.04	345.96		
	161.0	62.0			4.13	345.87		
	164.0	59.0			4.01	345.99		
	167.0	56.0			3.95	346.05		
	170.0	53.0			3.82	346.18		
	173.0	50.0			3.24	346.76		
	176.0	47.0			3.59	346.41		
	179.0	44.0			3.60	346.40		
TP	182.0	41.0			3.40	346.60		
			10.75	357.35				
	185.0	38.0			10.57	346.78		
	188.0	35.0			9.75	347.60		
	191.0	32.0			8.63	348.72		
	194.0	29.0			7.88	349.47		
	197.0	26.0			6.84	350.51		
	200.0	23.0			6.00	351.35		
	203.0	20.0			5.04	352.31		
	206.0	17.0			3.98	353.37		
	209.0	14.0			3.48	353.87		
	210.2	12.8			3.39	353.96		
	224.7	-1.7			3.54	353.81		

Cross Section H (23 April 2022)

BM / TP	STA from RB	STA from LB	BS+	HI	FS-	ELEV	WD	WSE
NGS BM NAVD88						356.20		
NGS BM NGVD27						353.51		
			3.81	357.32				
TP1					4.88	352.44		
			4.76	357.20				
BM XSH RB	9.2	222.8			4.10	353.10		
	30.0	202.0			3.93	353.27		
	45.0	187.0			8.42	348.78		
	55.0	177.0			11.78	345.42		
TP2	58.0	174.0			12.45	344.75		
			3.52	348.27				
	64.0	168.0			4.66	343.61		
	71.0	161.0			4.80	343.47		
	76.0	156.0			4.92	343.35		
HWM	83.0	149.0			4.45	343.82		
	91.2	140.8			5.11	343.16		
	102.0	130.0			6.78	341.49		
	106.0	126.0			7.71	340.56		
	108.3	123.8			7.98	340.29		
	116.0	116.0			7.38	340.89		
	126.8	105.2			8.09	340.18		
	131.0	101.0			8.24	340.03	0.30	340.33
	132.0	100.0			8.49	339.78	0.55	340.33
	133.0	99.0			8.88	339.39	0.95	340.34
	134.0	98.0			8.36	339.91	0.40	340.31
	134.5	97.5			8.13	340.14		
	137.5	94.5			7.80	340.47		
	140.0	92.0			6.90	341.37		
HWM	140.0	92.0			5.14	343.13		
HWM	138.0	94.0			5.07	343.20		
	142.7	89.3			5.84	342.43		
	147.1	84.9			3.95	344.32		
TP3	147.7	84.3			3.87	344.40		
	159.0	73.0			4.86	343.41		
	166.0	66.0			4.31	343.96		
			11.31	355.71				
	179.4	52.6			11.57	344.14		
	190.5	41.5			10.98	344.73		
	198.3	33.8			8.81	346.90		
	209.0	23.0			5.48	350.23		
	215.6	16.4			3.27	352.44		

Interstate 580 HWM Survey (23 April 2022)

BM / TP	STA	BS+	HI	FS-	ELEV	HWM	NOTES
NGS BM NAVD88					356.20		BM
NGS BM NGVD27					353.51		BM
		0.71	354.22				
TP1				13.04	341.18		just upstream from 9.9" on gage
		0.57	341.75				
TP2				6.14	335.61		
		4.80	340.41		341.75		
	6.0			5.00	336.75		channel (at right bank)
	6.0			3.50		338.25	HWM (on right bank)
	20.4			5.20	336.55		channel at XS
	20.4			3.44		338.31	HWM at XS
	40.0			5.46	336.29		channel
	40.0			3.38		338.37	HWM
	49.6			5.48	336.27		channel
	49.6			3.23		338.52	HWM
	49.6			3.44		338.31	HWM

Longitudinal Profile: upper reach south of Gleason Dr (18 Nov 2022)

BM/TP /HWM	STA	BS+	HI	FS-	ELEV	Water Depth	Water Elev	Upper Stadia	Lower Stadia	Stadia Dist	Level Heading	Δ Heading	Δ LP Dist	Σ LP Dist	NOTES
	0				360.18	0.64	360.82							0	Gleason toe of concrete apron (elev from Tompkins '05)
BM	0	3.36	363.54					3.40	3.34	6	51.0				
	1			4.37	359.17	1.65	360.82	4.44	4.30	14	58.0	7.0	8	8	
	2			5.23	358.31	2.50	360.81	5.40	5.05	35	51.0	353.0	21	29	
TP 1	2	6.83	365.14					6.92	6.75	17	53.0				
	3			6.34	358.80	2.00	360.80	6.36	6.31	5	63.0	10.0	12	41	
	4			8.06	357.08	2.60	359.68	8.12	8.00	12	231.0	168.0	17	58	
	5			8.26	356.88	2.40	359.28	8.35	7.14	121	230.0	359.0	109	167	
TP 2	5	5.41	362.29					6.64	6.20	44	176.0				
	6			3.91	358.38	0.36	358.74	4.01	3.81	20	174.0	358.0	24	191	riffle
	7			5.85	356.44	1.72	358.16	6.04	5.91	13	16.0	202.0	32	224	pool
	8			5.04	357.25	0.85	358.10	5.31	5.00	31	23.0	7.0	18	242	downstream from large willow
	9			7.46	354.83	2.80	357.63	7.65	7.26	39	28.0	5.0	9	250	pool
	10			6.39	355.90	1.72	357.62	6.68	6.10	58	30.0	2.0	19	270	
TP 3	10	4.99	360.89					5.25	4.73	52	10.0				
	11			5.54	355.35	0.90	356.25	5.61	5.51	10	179.0	169.0	62	331	grade control upper end
	12			5.51	355.38	0.98	356.36	5.65	5.40	25	179.0	0.0	15	346	grade control lower end
TP 4	12	5.16	360.54					5.50	4.82	68	209.0				
	13			5.32	355.22	1.11	356.33	5.44	5.21	23	196.0	347.0	46	392	
	14			5.05	355.49	0.52	356.01	5.21	4.91	30	353.0	157.0	52	444	
TP 5	14	3.16	358.65					3.24	3.06	18	263.0				
	15			3.70	354.95	0.35	355.30	3.90	3.59	31	43.0	140.0	46	490	at debris jam
HWM	15			1.08	357.57										top of debris jam
	16			4.38	354.27	0.97	355.24	4.61	4.15	46	43.0	43.0	46	536	
TP 6	16	3.45	357.72					3.68	3.22	46	119.0				
	17			3.76	353.96	0.49	354.45	3.85	3.67	18	121.0	2.0	28	564	upstream from XS B
	18			4.71	353.01	1.45	354.46	4.75	4.69	6	112.0	351.0	12	577	downstream from XS B
HWM	18			3.71	354.01										wash line at XS B, approximate
	19			4.47	353.25	1.20	354.45	4.63	4.33	30	296.0	184.0	36	613	
TP 7	19	5.45	358.70					5.55	5.02	53	161.0				
	20			5.47	353.23	1.20	354.43	5.70	5.24	46	14.0	213.0	95	708	upstream of waterfall
	21			8.16	350.54	2.57	353.11	7.82	7.22	60	16.0	2.0	14	722	downstream of waterfall
TP 8	21	7.75	358.29					7.83	7.68	15	56.0				move instrument to left bank (previously was in channel)
BM				4.22	354.07	0.10	354.17	4.31	4.11	20	62.0	6.0	-5	716	on wooden check dam at 107+00 - save as benchmark

Longitudinal Profile: lower reach Dublin Blvd to Interstate 580 (18 Nov 2022)

BM/TP /HWM	STA	BS+	HI	FS-	ELEV	Water Depth	Water Elev	Upper Stadia	Lower Stadia	Stadia Dist	Level Heading	Δ Heading	Δ LP Dist	Σ LP Dist	NOTES
	0				342.13	0.70	342.83							0	downstream end of Dublin Blvd underpass
BM	0	5.90	348.03					6.26	5.53	73	266.7				instrument on right bank
	1			5.54	342.49	0.10	342.59	5.73	5.36	37	277.5	10.9	37	37	edge of grade control
	2			6.83	341.20	1.10	342.30	6.96	6.70	26	282.0	4.5	11	49	
	3			6.34	341.69	0.60	342.29	6.41	6.26	15	301.0	19.0	13	61	
	4			6.80	341.23	1.06	342.29	6.88	6.73	15	34.0	93.0	22	83	
HWM	4			3.76	344.27										trash line at ^ station
	5			6.45	341.58	0.72	342.30	6.67	6.22	45	60.0	26.0	32	115	
	6			6.79	341.24	1.06	342.30	7.22	6.36	86	65.0	5.0	41	157	
TP 1	6	6.26	347.50					6.70	5.80	90	56.0				instrument on right bank
	7			6.89	340.61	1.70	342.31	7.06	6.69	37	60.0	4.0	53	210	
	8			7.04	340.46	1.85	342.31	7.14	6.94	20	74.0	14.0	18	228	
HWM	8			3.49	344.01										trash line at ^ station
	9			6.13	341.37	0.94	342.31	6.19	6.07	12	172.5	98.5	25	253	upstream of XS G
	10			5.63	341.87	0.45	342.32	5.71	5.54	17	200.0	27.5	8	261	on XS G
HWM	10			3.19	344.31										trash line at ^ station
	11			5.59	341.91	0.40	342.31	5.72	5.46	26	211.0	11.0	10	271	downstream of XS G
HWM	11			5.75	341.75										on inset sediment bar at ^ station
	12			5.55	341.95	0.38	342.33	5.79	5.31	48	220.0	9.0	23	294	at downstream end of sediment bar
	13			5.81	341.69	0.65	342.34	6.12	5.50	62	222.0	2.0	14	308	
HWM	13			3.30	344.20										trash line at ^ station
	14			5.39	342.11	0.12	342.23	5.75	5.02	73	224.0	2.0	11	319	riffle
TP 2	14	4.95	347.06					5.29	4.61	68	155.0				instrument on right bank
	15			5.50	341.56	0.60	342.16	5.79	5.23	56	157.0	2.0	12	331	pool
	16			5.17	341.89	0.10	341.99	5.43	4.91	52	158.0	1.0	4	336	riffle
	17			6.19	340.87	0.95	341.82	6.35	6.03	32	159.0	1.0	20	356	pool
	18			5.52	341.54	0.25	341.79	5.57	5.47	10	265.0	106.0	36	392	riffle
	19			6.49	340.57	1.22	341.79	6.62	6.37	25	305.0	40.0	18	410	pool
	20			5.76	341.30	0.48	341.78	5.95	5.53	42	312.0	7.0	17	428	riffle
	21			6.19	340.87	0.94	341.81	6.44	5.93	51	316.0	4.0	10	437	pool
	22			5.44	341.62	0.18	341.80	5.75	5.13	62	317.5	1.5	11	448	riffle
TP 3	22	4.50	346.12					4.98	4.03	95	32.0				
	23			4.85	341.27	0.50	341.77	5.32	4.41	91	33.0	1.0	4	453	
HWM	23			3.19	342.93		342.93								trash line at ^ station
	24			5.89	340.23	1.50	341.73	6.17	5.58	59	29.5	356.5	32	485	pool; bulrush downstream
HWM	24			2.92	343.20										trash line at ^ station
	25			6.13	339.99	1.74	341.73	6.33	5.96	37	37.0	7.5	23	508	pool
	26			6.04	340.08	1.63	341.71	6.09	5.98	11	64.0	27.0	28	535	upstream of bulrush
	27			4.80	341.32	0.39	341.71	4.89	4.72	17	145.0	81.0	19	554	riffle; downstream of bulrush
	28			4.81	341.31	0.41	341.72	4.94	4.67	27	170.5	25.5	14	568	
	29			5.20	340.92	0.80	341.72	5.37	5.03	34	177.5	7.0	8	576	
HWM	29			3.15	342.97										high water mark on floodplain
	30			5.00	341.12	0.58	341.70	5.21	4.80	41	185.0	7.5	9	584	downstream of bulrush
	31			5.37	340.75	0.89	341.64	5.71	5.04	67	192.0	7.0	27	611	pool
	32			4.91	341.21	0.28	341.49	5.32	4.50	82	196.0	4.0	16	627	riffle
TP 4	32	4.81	346.02					5.25	4.36	89	349.0				
	33			5.97	340.05	1.10	341.15	6.39	5.57	82	350.0	1.0	7	634	pool
	34			5.27	340.75	0.10	340.85	5.64	4.89	75	350.0	0.0	7	641	riffle
	35			8.20	337.82	2.60	340.42	8.54	7.90	64	351.0	1.0	11	652	dropoff
	36			7.09	338.93	2.44	341.37	7.18	7.03	15	123.0	132.0	75	727	big pool
	37			7.57	338.45	1.96	340.41	7.83	7.39	44	143.5	20.5	30	757	
TP 5	37	6.49	344.94					7.06	5.92	114	42.5				
	38			5.84	339.10	1.20	340.30	5.92	5.77	15	79.0	36.5	102	860	upstream of bulrush
	39			4.83	340.11	0.22	340.33	4.96	4.67	29	174.0	95.0	34	894	riffle, downstream of bulrush
	40			5.45	339.49	0.80	340.29	5.64	5.23	41	185.0	11.0	14	907	upstream of XS H
HWM	40			3.31	341.63										trash line at ^ station
	41			5.61	339.33	1.00	340.33	5.86	5.37	49	191.0	191.0	49	956	on XS H
HWM	41			3.79	341.15										trash line at ^ station
	42			5.03	339.91	0.19	340.10	5.28	4.76	52	196.0	196.0	52	1008	downstream of XS H
	43			6.20	338.74	1.38	340.12	6.55	5.87	68	204.0	8.0	18	1026	pool, downstream of bulrush
	44			5.05	339.89	0.10	339.99	5.44	4.66	78	208.0	4.0	11	1038	riffle
	45			7.67	337.27	1.95	339.22	8.09	7.23	86	210.0	2.0	8	1046	
TP 6	45	6.09	343.36					6.84	5.33	151	120.0				
	46			4.53	338.83	0.40	339.23	5.11	3.96	115	123.0	3.0	37	1083	riffle
	47			5.31	338.05	1.10	339.15	5.81	4.81	100	124.5	1.5	15	1098	pool
	48			4.47	338.89	0.10	338.99	4.93	3.99	94	127.0	2.5	7	1105	riffle
	49			5.96	337.40	1.18	338.58	6.38	5.55	83	127.5	0.5	11	1116	pool
	50			5.02	338.34	0.20	338.54	5.29	4.75	54	134.0	6.5	30	1146	riffle
	51			6.16	337.20	0.95	338.15	6.37	5.94	43	137.0	3.0	11	1158	pool; cobble/boulder bed
	52			6.85	336.51	1.62	338.13	6.93	6.77	16	166.0	29.0	30	1188	pool
	53			7.12	336.24	1.90	338.14	7.25	6.99	26	281.0	115.0	36	1223	
	54			7.35	336.01	2.20	338.21	7.68	7.08	60	285.0	4.0	34	1258	pool
	55			5.52	337.84	0.26	338.10	5.92	5.13	79	285.0	0.0	19	1277	riffle
	56			6.73	336.63	1.46	338.09	7.23	6.23	100	289.0	4.0	22	1298	pool
	57			5.50	337.86	0.20	338.06	5.24	4.74	50	290.0	1.0	50	1348	riffle
	58			8.65	334.71	2.95	337.66	9.60	7.95	165	290.0	0.0	115	1463	pool
	59			5.85	337.51	0.12	337.63	6.78	4.90	188	290.0	0.0	23	1486	upstream end of concrete apron at I-580 frontage road
HWM	59			4.72	338.64										debris buildup on concrete apron